Phase I and phase II metabolism simulation of antitumor-active 2-hydroxyacridinone with electrochemistry coupled on-line with mass spectrometry.

Journal:	*Xenobiotica*
Manuscript ID	TXEN-2018-0223.R1
Manuscript Type:	Original Article
Keywords:	in vitro metabolism, metabolic activation, electrochemical oxidation, electrochemistry-mass spectrometry, metabolite electrosynthesis, reactive metabolite, glutathione S-conjugate

Title:

Phase I and phase II metabolism simulation of antitumor-active 2-hydroxyacridinone with electrochemistry coupled on-line with mass spectrometry.

Abstract

1. Here, we report the metabolic profile and the results of associated metabolic studies of 2-hydroxyacridinone (2-OH-AC), the reference compound for antitumor-active imidazo- and triazoloacridinones.
2. Electrochemistry coupled with mass spectrometry was applied to simulate the general oxidative metabolism of 2-OH-AC for the first time. The reactivity of 2-OH-AC products to biomolecules was also examined. The usefulness of the electrochemistry for studying the reactive drug metabolite trapping (conjugation reactions) was evaluated by the comparison with conventional electrochemical (controlled-potential electrolysis) and enzymatic (microsomal incubation) approaches.
3. 2-OH-AC oxidation products were generated in an electrochemical thin-layer cell. Their tentative structures were assigned based on tandem mass spectrometry in combination with accurate mass measurements. Moreover, the electrochemical conversion of 2-OH-AC in the presence of reduced glutathione and/or *N*-acetylcysteine unveiled the formation of reactive metabolite-nucleophilic trapping agent conjugates (*m/z* 517 and *m/z* 373, respectively) via the thiol group. This glutathione S-conjugate was also identified after electrolysis experiment as well as was detected in liver microsomes.
4. Summing up, the present work illustrates that the electrochemical simulation of metabolic reactions successfully supports the results of classical electrochemical and enzymatic studies. Therefore, it can be a useful tool for synthesis of drug metabolites, including reactive metabolites.

Keywords:

in vitro metabolism; metabolic activation; electrochemical oxidation; electrochemistry-mass spectrometry; metabolite electrosynthesis; reactive metabolite; glutathione S-conjugate;

Introduction

Solid understanding of the metabolic pathways and the biotransformation mechanisms of new drug candidates is a crucial point in the drug discovery and development processes. Overall, it allows to elucidate the metabolic activation as well as the deactivation routes of new biologically active compounds, especially in respect to their possible toxicity (Park *et al.* 2011). The identification of metabolites helps to eliminate the inappropriate candidates at an early stage, before the more expensive development phases will be performed (Bussy & Boujtita 2014). Particularly, it is very important that the formation of chemically reactive intermediates is checked (Baillie *et al.* 2002), because an increasing number of reports indicate that they are responsible for the majority of rapid and unexpected drug toxic effects (Kalgutkar & Soglia 2005; Srivastava *et al.* 2010; Orhan & Vermeulen 2011). The relationship between drug metabolism and adverse drug reactions was first demonstrated with the analgesic agent acetaminophen (Jollow *et al.* 1973; Larson 2007). Reactive intermediates, generated usually via cytochrome P450 (P450)-catalyzed oxidative reactions, have the potential for covalent binding to cellular nucleophiles such as purine and pyrimidine bases of DNA or thiols of proteins, and form stable adducts. Adduct formation may alter biological functions of these biomolecules what ultimately leads to a toxic response (Brandon *et al.* 2003).

Metabolic activation of new drugs to reactive intermediates is currently assessed in the presence or the absence of reactive endogenous nucleophiles, such as reduced glutathione (GSH), *N*-acetylcysteine (NAC) or β-lactoglobulin A (βLGA), a model protein. In practise, the reaction usually involves the *in vitro* incubation of a studied compound with an excess of the selected chemical-trapping agent in hepatocytes or liver microsomes (as a source of cytochrome P450 isoenzymes). *In vivo* experiments involve laboratory animals (Kalgutkar & Soglia 2005). However, performing these biological schemes is usually laborious and time-consuming. Despite continuous improvements in metabolite-identification tools, the identification of some reactive metabolites remains difficult due to the matrix complexity, low concentration or their binding to matrix bio-components (Bussy *et al.* 2015). Isolated

hepatocytes have only a very limited proliferative potential *in vitro* and a correspondingly short life-span in primary culture. Their fenotype is unstable and the level and activities of enzymes, such as cytochromes P450, fall quickly in a few days (Jennings & Strauss 1999). Also liver microsomes offer a limited reproducibility. Additionally, because of genetic polymorphisms, variations in the gene expression for individual drug-metabolising izoenzymes in each organism have to be taken into account (Pinto & Dolan 2011; Zanger & Schwab 2013).

As an alternative to the existing methods for studies on drug metabolism and toxicity, the electrochemical simulation of P450-catalyzed phase I reactions, mostly initiated by a single-electron transfer, has been developed (Volk *et al.* 1992; Lohmann & Karst 2008; Faber *et al.* 2011). Overall, it allows to simulate a wide variety of oxidation-reduction (redox) processes occurring in living organisms (Jurva *et al.* 2003; Nouri-Nigjeh *et al.* 2011). The combination of electrochemistry (EC) coupled on-line with mass spectrometry (MS) creates a powerful platform for rapid generation (in the electrochemical cell) and detection (by mass spectrometry) of a series of metabolic products, including observation of reactive metabolites (Permentier *et al.* 2008; Faber *et al.* 2011; Bussy & Boujtita 2014). Use of EC/MS improves the conventional methods of drug metabolism studies. It is a purely instrumental technique with a simple set-up that enables the generation of drug metabolites in the absence of biological matrices in the reaction medium. So, the application of EC/MS helps to overcome many of the laborious tasks related to isolation and identification of metabolic products formed *in vitro* (cultured hepatocytes, liver microsomes, purified enzymes) or *in vivo* (urine, plasma, *etc.*) (Orhan & Vermeulen 2011; Faber *et al.* 2011). Moreover, on-line combining EC with MS can provide valuable information about metabolically labile sites in a drug molecule and predict its reliable metabolic profile in a much shorter time (Jurva *et al.* 2003; Permentier *et al.* 2008).

Recently extensive research have been conducted in our group to determine the possible metabolic pathways of potential antitumor drugs and their model compounds. The objective of the investigations presented here was to develop and evaluate an on-line EC/MS method

for the simulation of oxidative metabolism of 2-hydroxyacridinone (2-OH-AC) (a structure in the frame in Figure 1), a simple reference compound for high antitumor-active imidazo- and triazoloacridinones.

The preliminary studies in this field were performed earlier by the application of cyclic voltammetry, spectroelectrochemical measurements, and controlled-potential electrolysis (Mazerska *et al.* 1997, 2002). These experiments indicated the ability of 2-OH-AC to undergo oxidative metabolic activation in the living organism. However, no data for acridinone derivatives are yet available using the direct coupling EC with MS. The studies presented here were undertaken with respect to the usefulness of EC/MS technique for futher investigation on the oxidative metabolic activation and the identification of potential reactive metabolites formed during the metabolism of antitumor-active imidazoacridinone C-1311 and triazoloacridinone C-1305. These compounds, developed in our laboratory, have demonstrated significant cytotoxic and antitumor activities (Cholody *et al.* 1990, 1996; Kusnierczyk *et al.* 1994). The data obtained so far indicate that they have different spectrum of antitumor activity and exhibit various mechanisms of action at the molecular level (Dziegielewski & Konopa 1996; Skladanowski *et al.* 1996; Dziegielewski *et al.* 2002; Lemke *et al.* 2005; Augustin *et al.* 2006). Metabolic activation is the leading concept for the reason how imidazo- and triazoloacridinone derivatives cause high antitumor effect (Dziegielewski & Konopa 1998; Mazerska *et al.* 2001; Koba & Konopa 2007). It is assumed that the hydroxyl group in the acridinone ring provides the susceptibility of these compounds to oxidative metabolism. The formation of the intermediate, characterized as a quinone imine structure, that expresses antitumor activity, has been shown, for example, in the case of 9-hydroxyellipticine (Harding & Grummitt 2003). A known quinone imine with activity against human tumor cells is actinomycin D (Marks & Venditti 1976).

In this work, the ability of EC/MS to expedite the generation and identification of the main phase I metabolites of 2-OH-AC will be discussed. The formation of the reactive 2-OH-AC intermediate metabolite and the possibility to simulate its covalent binding to biomolecule (*i.e.*, glutathione (GSH) and/or *N*-acetylcysteine (NAC) as biomarkers of metabolic activity;

phase II metabolism) are also taken into account. Furthermore, to show the capability of electrochemistry to simulate certain P450-mediated reactions, the results obtained by EC were also compared with those gained after controlled-potential electrolysis (CPE) and conventional *in vitro* studies by conducting incubations of 2-OH-AC with human and rat liver microsomes (HLMs and RLMs, respectively). The products of electrolysis and enzymatic transformations of 2-OH-AC were analysed by reversed-phase liquid chromatography (LC) with UV-Vis detection and/or diode array detection, and monitored by MS. The relation between the products generated electrochemically and enzymatically for the model compound 2-OH-AC can provide a clue to the nature of their metabolic pathway initiation (Volk *et al.* 1992). It opens up further perspectives directed to the search for more effective and less toxic antitumor drugs among acridinone derivatives. It is significant because improves the risk evaluation for potential drugs in the optimal chemotherapy schedules designed for individual patients.

List of abbreviations:

CPE, controlled-potential electrolysis;

CV, cyclic voltammetry, cyclic voltammogram;

EC, electrochemistry, electrochemical cell;

ESI, electrospray ionization;

GC, glassy carbon;

GSH, glutathione (reduced form);

HLMs, human liver microsomes;

2-OH-AC, 2-hydroxyacridinone;

m/z, mass-to-charge ratio;

MS, mass spectrometry, mass spectrometer;

MS/MS, tandem mass spectrometry;

NADPH, β-nicotinamide adenine dinucleotide 2'-phosphate tetrasodium salt (reduced form);

NAC, *N*-acetylcysteine;

P450, cytochrome P450;

PBS, phosphate-buffered saline;

Q-TOF, quadrupole-time of flight;

RLMs, rat liver microsomes;

LC, liquid chromatography;

Parts of this work were presented at the 13th European ISSX Meeting (Glasgow, Scotland, 2015) and at the 2nd Congress BIO 2016 (Wrocław, Poland, 2016).

Materials and methods

Chemicals and enzymes

An acridinone derivative, a 2-hydroxyacridinone (2-OH-AC) was synthesized in our laboratory according to the method described earlier (Acheson 1973). The following chemicals were purchased from Sigma-Aldrich (St. Louis, MO, USA): *N*-acetylcysteine (NAC), dipotassium phosphate (K_2HPO_4), disodium phosphate (Na_2HPO_4), formic acid (HCOOH), L-glutathione reduced (GSH), monopotassium phosphate (KH_2PO_4), monosodium phosphate (NaH_2PO_4), and semicarbazide hydrochloride. Methanol (gradient grade for liquid chromatography) and *β*-nicotinamide adenine dinucleotide 2'-phosphate tetrasodium salt (*β*-NADPH) were obtained from Merck KGaA (Darmstadt, Germany). Ammonium formate ($HCOONH_4$) was ordered from Fisher Scientific (Loughborough, UK). Aluminum oxide (Al_2O_3) powder in form of 1-µm alumina suspension, for polishing of electrodes, was delivered by TESTING Sp z o.o. (Katowice, Poland). All other commercially available chemicals and reagents were of the highest possible grade available. Ultrapure water (0.056 $\mu S \cdot cm^{-1}$), used in all the experiments, was passed through a Milli-Q water purification system from Merck KGaA (Darmstadt, Germany) or water distillation system from Hydrolab Sp. z o.o. sp.k. (Straszyn, Poland).

Pooled human liver microsomes (HLMs), mixed gender, from 50 donors (protein concentration, 20 $mg \cdot mL^{-1}$; P450 content, 411 $pmol \cdot mg^{-1}$ protein) and pooled rat liver microsomes (RLMs) from untreated, male Sprague-Dawley rats (protein concentration, 20 $mg \cdot mL^{-1}$; P450 content, 680 $pmol \cdot mg^{-1}$ protein) were purchased from Tebu-bio (Le Perray-En-Yvelines, France).

General instrumentation

Electrochemical measurements

Electrochemical measurements of the oxidation-reduction properties of 2-OH-AC were performed with controlled-potential electrolysis (CPE) and by electrochemical metabolism simulation in a three-electrode thin-layer cell (EC).

CPE was performed using an Autolab (Eco Chemie B.V., Utrecht, The Netherlands), model PGSTAT 12 potentiostat, controlled via producer's software. The three-electrode system, consisting of a cylinder glassy carbon (GC) working electrode (ϕ = 3 mm and 13 mm long; A = 1.296 cm^2), an Ag/AgCl/3 M KCl reference electrode and a platinum-wire counter electrode, were employed. During chronoamperometric measurements the working electrode as well as the analyzed solution were placed in a glass tube closed with a "Vicor" plug to separate the electrolyzed solution from the main solution.

Simulation of the oxidative metabolism reactions of 2-OH-AC was accomplished in an electrochemical thin-layer cell equipped with a disc glassy carbon (GC) working electrode (ϕ = 8 mm; A = 0.502 cm^2) and a Pd/H_2 reference electrode (reactor cell; Antec Leyden, Zoeterwoude, The Netherlands). Carbon-loaded PTFE (polytetrafluoroethylene) served as auxiliary electrode. The cell potentials were applied using a ROXY EC System (Antec Leyden) controlled by Antec Dialogue software (Antec Leyden). The outlet of the electrochemical cell was connected directly to an electrospray ionization (ESI) source of a quadrupole-time of flight (Q-TOF) mass spectrometer (Agilent Technologies, Santa Clara, CA, USA) (Figure 1a). S-Conjugate formation of 2-OH-AC and GSH (NAC) was established using a T-piece and a 100 µL mixing coil placed between reactor cell and the ESI source (Figure 1b). The relevant EC conditions can be viewed in Table 1.

Liquid chromatographic analyses

For all analyses of 2-OH-AC, liquid chromatographic (LC) separations were performed on a reversed-phase 5-µm Suplex pKb-100 analytical column (4.6 mm x 250 mm, C18) (Supelco Inc., Bellefonte, PA, USA) with Waters Associates HPLC system (Waters Co., Milford, MA, USA). It was equipped with a model 600E system controller, a model 7725i Rheodyne injector, and a model 2996 photodiode array detector (DAD) controlled with Millennium software (Waters Co.). The LC analyses were carried out at a flow rate of 1 $mL \cdot min^{-1}$ with the following mobile phase system: a linear gradient from 15% to 80% methanol in 0.05 M aqueous ammonium formate buffer (pH 3.40 adjusted with formic acid)

for 25 min, followed by a linear gradient from 80% to 100% methanol in ammonium formate buffer, pH 3.40, for 3 min. The eluates were monitored at 380 nm.

Mass spectrometry

Mass spectrometric detection, identification, and fragmentation of 2-OH-AC products were carried out in the positive-ion mode by recording full scan spectra (*m/z* 100 – 600). To ensure accurate mass during the experiment, the mass spectrometer was calibrated on a daily basis, prior to sample analysis. The corresponding conditions for the ESI-Q-TOF-MS(/MS) measurements are listed in Table 1.

Controlled-potential electrolysis of 2-OH-AC

The controlled-potential electrolysis was performed in 0.02 M phosphate-buffered saline (PBS), pH 7.40, obtained by mixing Na_2HPO_4 and KH_2PO_4, and adding the appropriate amounts of NaCl and KCl to reach their concentrations of 0.15 and 0.002 M, respectively. Each time before the electrolysis experiments the GC working electrode was briefly polished with 1-µm Al_2O_3 powder on a wet pad. After polishing step, to remove alumina completely from the surface, the electrode was rinsed with a direct stream of ultrapure water. To eliminate the electric noise the electrochemical cell was placed in a Faraday cage. The chronoamperometric experiments of 0.5 mM 2-OH-AC in the absence and the presence of 10-fold excess of GSH were performed at 0.50 V. The electrolysis progress was monitored by voltammetric, spectroscopic, chromatographic, and spectrometric methods. The experiments have been performed at room temperature (21 ºC).

Electrochemical simulation of the oxidative metabolism of 2-OH-AC

For the electrochemical conversion, a 10-µM 2-OH-AC solution in electrolyte (0.1% formic acid in water/methanol, 50/50, *v/v*) was pumped (SP2 – ROXY dual piston syringe pump; Antec Leyden) through the electrochemical cell at a constant flow rate of 30 $\mu L \cdot min^{-1}$. The potential of working electrode in the reactor cell was ramped between 0 and 2500 mV (scan rate 10 $mV \cdot s^{-1}$). The outlet of the reactor cell was connected on-line to the ESI-MS source (Figure 1a). To identify potential aldehyde products the oxidized sample was collected in a vial containing semicarbazide (dissolved in ultrapure water) to give a final

concentration of 5 mM. After collection, the samples from the trapping experiments were kept at 25 ºC for 1 h before analysis by LC/MS.

The properties of the sample solvent may influence the conversion efficiency in the electrochemical cell. Therefore, the electrochemical simulation of the oxidative metabolism of 2-OH-AC has been also performed in two different electrolyte solutions containing acetonitrile (0.1% formic acid or 20 mM ammonium formate (pH 3.40), respectively, in water/acetonitrile, 50/50, *v/v*).

On-line trapping of oxidation product with glutathione (N-acetylcysteine)

To identify possible S-conjugate(s) with GSH (NAC), the EC/MS set-up described above was slightly modified (Figure 1b). A 10-µM 2-OH-AC solution in electrolyte was pumped through the electrochemical cell at a constant flow rate of 30 µL·min^{-1}. 100 µM GSH (NAC) in ultrapure water was added at the same flow rate to the effluent of the electrochemical cell via a T-piece into a 100 µL mixing coil. The effluent from the mixing coil was injected directly into the ESI-MS interface.

In vitro microsomal incubations

Human or rat liver microsomal incubations (1 mg·mL^{-1} protein) were performed with 50 µM 2-OH-AC, 1 mM NADPH, and 1 mM GSH in a potassium phosphate-buffered solution (0.1 M, pH 7.40) at 37 °C for 1 h, in a total volume of 100 µL. The incubations were terminated by adding ice-cold methanol to the incubation mixtures (50:50, *v/v*). The samples were then vortexed, placed in ice for 10 min, and centrifuged at 10000 x g for 10 min. Aliquots of the supernatants (150 µL) were then analyzed directly by reversed-phase LC with UV-Vis detection and/or diode array and multiple wavelength detection, and monitored by MS. The three types of control incubations were applied, the first without test compound, the second without NADPH, and the third without GSH.

Results

In order to provide an important insight into the mechanism of antitumor action of imidazo- and triazoloacridinones, the electrochemical oxidation of their simpler reference compound,

2-OH-AC, was investigated. The ability of 2-OH-AC to undergo oxidative metabolic activation was studied by applying the direct combination of electrochemistry and mass spectrometry (EC/MS). For 2-OH-AC no EC/MS data were found before. Electrochemical conversion of 2-OH-AC was conducted in parallel to controlled-potential electrolysis (CPE) and *in vitro* experiments using liver microsomes.

Controlled-potential electrolysis of 2-OH-AC

At first, cyclic voltammetry (CV) was used to initially investigate the electrochemistry of 2-OH-AC at a glassy carbon electrode in a range of positive potentials and to determine the optimum operating range of voltages for further EC/MS studies. In order to confirm the postulated oxidation mechanism of 2-OH-AC action and to identify the oxidation products, controlled-potential electrolysis of 2-OH-AC (0.5 mM in 0.02 M PBS buffer, pH 7.40) was performed at 0.50 V. To support the possibility of the formation of the stable adduct between 2-OH-AC intermediate and GSH, the tests were performed in the absence and the presence of GSH (5 mM in ultrapure water). The electrolysis measurements were carried out for 24 hours and the progress of the process was monitored periodically by application of voltammetric, spectroscopic, chromatographic, and spectrometric methods.

Data for the CV are provided in the supplemental material. In the solution of pure 2-OH-AC one anodic peak (a1) and three cathodic peaks (c1, c2, c3) were obtained. The appearance of three cathodic peaks indicated that the oxidation product of 2-OH-AC underwent subsequent chemical reactions. The addition of 10-fold excess of GSH to 2-OH-AC solution resulted in a shift of the oxidation peak of 2-OH-AC of about 30 mV to a more positive potential. In turn, the signal appearing in the cathodic part of the CV at circa 0.32 V virtually disappeared and two other cathodic peaks were substantially depressed. These

changes confirmed the interaction between 2-OH-AC and GSH, and the reducing effect of GSH against the oxidation reaction products.

Assuming that during oxidation process of 2-OH-AC two electrons are exchanged, the total electrolysis of 0.5 mM compound should be achieved at the time of obtaining the charge of 200 mC. Unfortunately, despite long electrolysis (over 1 day) the maximum charge which was achieved was only 29 mC. A possible explanation of this situation is that the oxidation products of 2-OH-AC strongly adsorbed on the electrode surface and effectively blocked it. With electrolysis progress the intensity of the current signals drastically decreased (Figure 2a). In addition, a new oxidation signal at circa 0.06 V (a2) was also well visible. It was related to the third cathodic peak (c1). The introduction of GSH to the solution of 2-OH-AC significantly minimized the effects of the electrolysis process. This observation may point out the presence of interactions between oxidation products of 2-OH-AC and GSH. The CPE of a mixture of 2-OH-AC and GSH (Figure 2b) revealed the anodic signal at circa 0.42 V (a1) with increasing intensity. Also a new signal emerged at circa 0.31 V (a2) and its height increased with time of electrolysis. This product peak was due to the reduction of the transformed 2-OH-AC molecule.

Electrochemical simulation of the oxidative metabolism of 2-OH-AC (phase I metabolism)

The electrochemical oxidation products of 2-OH-AC were generated and identified using on-line EC/MS (Figure 1a). The applied set up enabled us to simulate metabolic P450-catalyzed reactions occurring in the liver. To reduce the complexity of the system these experiments were carried out only with flow injection EC/MS without using an LC column.

The best electrochemical conversion of 2-OH-AC into its expected products was achieved using the scan mode in the potential range of 0 – 2.5 V. To provide a concise overview of the oxidation products, 2-D mass voltammograms were generated by plotting the extracted ion intensities versus the progress of the electrochemical oxidation. Mass spectrometry allowed the identification of the formed products by an increasing signal intensity of the corresponding mass-to-charge (*m/z*) ratio. Furthermore, for structure

elucidation of the detected products, fragment ions, generated by in-source fragmentation in the ESI interface, have been studied.

A representative 2-D mass voltammogram resulting from the oxidation of 2-OH-AC within the scanned range is shown in Figure 3. The 2-OH-AC molecule was easily protonated and detected with high intensities as $[M+H]^+$ ion (*m/z* 212) in the positive ionization mode of the ESI-Q-TOF mass spectrometer. No products were observed in the solution of pure 2-OH-AC without any electrochemical potential (cell off) (the inset of top left corner in Figure 3), whereas significant drop in an extracted ion intensity of 2-OH-AC was noticed when the potential was applied (cell on) (the inset of top right corner in Figure 3). This change is attributed to the oxidation of 2-OH-AC into eight products in an electrochemical thin-layer cell. All products are summarized in Table 2 and will be discussed in detail, with specific reference to their accurate mass data and fragmentation patterns.

Furthermore, we noticed that the ratios of oxidation products of 2-OH-AC were strongly dependent on the solvent composition. Most products identified using methanol-containing electrolyte, with the exception of P4 (*m/z* 240) and P8 (*m/z* 421), have been also observed in solutions of acetonitrile. No additional oxidation products of 2-OH-AC were detected under these conditions. Higher signal intensity of the selected mass ions was caused by that methanol was better than acetonitrile in diminishing the adsorption of the electrochemical products on the surface of the working electrode. Moreover, methanol/water electrolyte solution produced the lowest mass background noise in positive total ion chromatogram (data not shown). A summary of the electrochemical products observed under different electrolyte conditions is available in the supplemental material.

Characterization of GSH conjugate formed from electrochemical oxidation of 2-OH-AC (phase II metabolism)

In this work, the EC/MS set-up described above was extended to a system allowing the study of the conjugation of 2-OH-AC oxidation products with a reactive endogenous nucleophile, such as reduced GSH or NAC. GSH and NAC were selected because of a simple structure with their soft nucleophilic thiol group and their relevance in living organisms

(Evans *et al.* 2004). The instrumental set-up for electrochemical simulation of conjugation reactions (phase II reactions) is shown in Figure 1b.

Observation of the potential conjugation reaction(s) between the oxidation product(s) of 2-OH-AC and GSH was possible in the form of a 2-D mass voltammogram (Figure 4a).

The mass spectra were acquired to confirm the formation of GSH S-conjugate (Figure 5). As expected, no additional signals besides those associated with protonated 2-OH-AC (*m/z* 212) and GSH (*m/z* 308) were observed at cell off (Figure 5a and a zoom in the mass spectrum from the circle range). However, in the potential range of 0 – 2.5 V (cell on) mass spectrum revealed one *m/z* signal representing potential GSH S-conjugate (Figure 5b and a zoom in the mass spectrum from the circle range). Ion with a *m/z* ratio of 517 was observed with a weak intensity which was increasing only in the case when an extracted ion intensity of protonated 2-OH-AC was decreasing. It was confirmed by the accurate mass measurements that *m/z* 517 represents the conjugate of molecular formula $C_{23}H_{24}N_4O_8S$, consistent with a product of the 2-OH-AC oxidation and one molecule of GSH. This result is in accordance with the assumption that GSH traps soft electrophiles with its thiol group (Inoue *et al.* 2015).

To confirm that the ion at *m/z* 517 is originating from GSH conjugate of 2-OH-AC, the fragmentation spectrum was recorded (Figure 5c). The MS/MS of *m/z* 517 ion produced two fragment ions at *m/z* 388 and 244, respectively. The accurate values of *m/z* correlated well with calculated *m/z* (Table 3). The first was consistent with the neutral loss of anhydroglutamic acid (-129), whereas the second (-275) was assigned as a cleavage adjacent to the cysteinyl thioether moiety with charge retention on the 2-OH-AC molecule. Thus, the fragmentation pattern of *m/z* 517 ion suggested the presence of at least one GSH moiety. As for GSH, formation of NAC S-conjugate with a *m/z* ratio of 373 was also observed in similar experiments (Figure 4b). The MS/MS of 373 ion revealed the presence of the fragment ion at *m/z* 244 (data not shown), exactly the same that occurred in MS/MS of *m/z* 517 ion.

Identification of GSH conjugate of 2-OH-AC from in vitro microsomal incubations and controlled-potential electrolysis

Trapping experiments with GSH in *in vitro* microsomal incubations and during controlled-potential electrolysis of 2-OH-AC were carried out to generally assess the feasibility of GSH S-conjugate formation. The results obtained from these approaches were compared with those from a purely instrumental electrochemical simulation. Figure 6a presents the representative high performance LC chromatograms recorded for enzymatic and electrochemical oxidation of 2-OH-AC in the absence and the presence of 10-fold excess of GSH.

Due to various expressions of the different isoforms of P450 in each organism, the metabolism in human and rat liver microsomes may result in different metabolites or in a different quantitative distribution of the metabolites (Martignoni *et al.* 2006). When experiments were performed using both types of microsomal fractions, in the case of 2-OH-AC we observed only slight differences in the intensity of the individual peaks, hence the further discussion will be based on the results from RLM studies. The microsomal incubations included three controls, one without 2-OH-AC to rule out any potential interference/contamination from endogenous compounds, the second without NADPH, a cofactor for cytochrome P450 activities, to assess the metabolic dependence of GSH conjugate formation, and the third without GSH. No conjugate was detected in the "no compound' and "no NADPH" control reactions (data shown in the supplemental material). LC analysis of microsomal samples without GSH revealed that three main metabolites were formed under the conditions studied (Figure 6a). Chromatogram taken after 60 min incubation of 2-OH-AC with 10-fold excess of GSH represents one additional chromatographic peak. It is noteworthy that it was not seen in the control incubations without NADPH, which suggests an NADPH-dependent oxidation of 2-OH-AC to this metabolite**.** LC analysis of the reaction mixture throughout the course of controlled-potential electrolysis revealed one main product (Figure 6a). Compared to enzymatically generated metabolites,

two of them were missing. As before, one additional peak was observed only where GSH was present in excess, and its intensity depended on the progress of electrolysis.

In both approaches the UV-Vis spectra of the peaks at 18.6 min differed significantly from that of the substrate (the inset in Figure 6a). The shift towards longer wavelengths may indicate that a more extensive delocalized electron system exists in this product in comparison to that in 2-OH-AC. It was subsequently identified by ESI-MS as GSH S-conjugate with the mass ion at *m/z* 517 (data not shown). Therefore, the above results agreed with the data obtained from EC/MS or EC/MS/MS measurements and confirmed the existence of a reactive intermediate in the oxidative pathway of 2-OH-AC. However, due to the low concentration of the S-conjugate in the EC/MS system it was not possible to obtain its chromatographic peak and UV-Vis spectrum. Also other products showing quite good intensities in the EC/MS system, were found in small or trace amounts in LC analysis (Figure 6b). Some of them were not detected, which is likely to be a consequence of their low stability. Nevertheless, it is worth to note that generally the EC system allowed to obtain a wider set of phase I metabolites than the use of classical approaches, probably because of clean matrix.

Discussion

The toxic effects of drugs and other xenobiotics arise not only from the compound itself but also from its metabolites (Baumann *et al.* 2010). Hence, during drug development process particular attention is paid to drug metabolite formation and identification of metabolic pathways. Progress in this research area depends critically on the improvement of methods involved in the generation and analysis of various types of drug metabolites, with special respect to the characterization of reactive metabolites (Prakash *et al.* 2008). In this work different approaches for the investigation of the 2-OH-AC oxidative metabolism, that may occurs in the living organism, were performed. The oxidative electrochemical behavior of 2-OH-AC was first investigated by the direct combination of electrochemistry and mass spectrometry. The applicability of the electrochemistry in drug metabolite synthesis was evaluated by conventional electrochemical (controlled-potential electrolysis) and enzymatic (microsomal incubation) approaches.

The electrochemical conversion of 2-OH-AC in an electrochemical thin-layer cell was successfully achieved (Figure 3). Table 2 consists of list of major products related to 2-OH-AC oxidative metabolism and *m/z* ratios of the protonated species $[M+H]^+$ used for mass spectra interpretation. The resulting molecular formulas were deduced by their accurate masses. The isotopic patterns correlated well with theoretical calculations. For all compounds, the deviations between the calculated and measured *m/z* values were less than 4 ppm.

The proposed chemical reactions that may occur in the electrochemical cell are summarized in Figure 7. Most of 2-OH-AC oxidation products seem to be species containing additional oxygen atom and can exist in at least two tautomeric forms. According to previous studies on the oxidative transformations of 2-OH-AC (Mazerska *et al.* 2002), the most likely oxidation site in the 2-OH-AC molecule is the position *ortho* to the hydroxyl group. This relates to the positions 1 or 3 of 2-OH-AC, wherein position 1 remains preferential. Thus, the mass ion at *m/z* 226 is proposed to correspond to 1,2-orthoquinone (P1a), while the signal at *m/z* 228 may include monohydroxylation product (P3). The molecular ion observed with little

signal intensity at *m/z* 421 was identified to be the dimer formed from two substrate molecules of radical structure linked together at position 1 of 2-OH-AC (P8). The chemical structures of these three products have been previously determined by means of MS and NMR spectroscopy (Mazerska *et al.* 2002).

Other products of oxidative metabolism of 2-OH-AC have been identified for the first time upon electrochemical oxidation. The P2 compound with the mass ion at *m/z* 227 may have been formed via *C*- or *N*-hydroxylation because the mass corresponds to an addition of 15.99 Da to the parent compound with a lack of one hydrogen atom. As a result, the P2 molecule should contain a positive charge, probably located on the nitrogen atom of the acridinone ring. Further, considering the mesomeric effects in electron density distribution, the loss of one hydrogen atom in P2 compound would indicate the possibility of the formation other than P1a structures for the mass ion at *m/z* 226, including P1b.

The products showing the mass ions at *m/z* 240 (P4), 242 (P5), 256 (P6), and 258 (P7) have not been definitively identified. However, we propose here only their tentative structures. The accurate mass of ion at *m/z* 242 (P5) differed from the accurate mass of ion at *m/z* 226 (P1) by exactly 16.03 Da. This value may indicate the presence of the additional one carbon and four hydrogen atoms, but not a single oxygen atom (15.99 Da), somewhere within the P5 molecule. During the electrochemical and/or the ionization processes some side reactions can take place, like the reaction of electrolyte components with electrochemically generated intermediates and sometimes they are unexpected. Based on the literature data (Sichilongo *et al.* 2011; Wang *et al.* 2011), electro-oxidation of methanol from electrolyte may give a strongly electrophilic methylium (CH_3^+) or methyl radical ($\bullet CH_3$). Thus, we can assume that it is quite likely that compound containing a methyl group in its structure was formed. The probable methylation of 2-OH-AC derivative have not been avoided even when acetonitrile was present in the electrolyte solution (supplemental material). The possible location of attachment is speculated to be an electronegative nitrogen atom due to valence considerations. Presumably further two-electron two-proton dehydrogenation of P5 provided P4 (*m/z* 240), with molecular mass ion decreased by 2.01

Da. In turn, a product with the mass ion at *m/z* 258 (P7) could have been created by the hydroxylation of the methyl group of P5, and its further two-electron two-proton dehydrogenation gave a signal at *m/z* 256 (P6).

It should be pointed out that the signals at *m/z* 240 and *m/z* 256 may correspond to aldehyde products as well. To test whether the hydroxymethyl group at the nitrogen atom in P5 or in P7 products underwent further oxidation, trapping experiments were performed with semicarbazide. It is a small molecule trapping agent that can form a Schiff base with aldehydes in the process mimicking reactions between aldehyde metabolites with lysine residues on proteins (Evans *et al.* 2004). Semicarbazide was added to the electrochemical oxidation mixture of 2-OH-AC followed by LC/MS analysis. Trapping with semicarbazide did not give any conjugates what excluded the presence of aldehyde products in oxidative transformations of 2-OH-AC.

To simulate the phase II metabolism of 2-OH-AC, electrochemical oxidation of the compound was carried out in the presence of an excess amount of nucleophilic trapping agent. EC/MS successfully predicted the formation of chemically reactive metabolite that spontaneously reacted with reduced glutathione (Figures 4a and 5) and/or *N*-acetylcysteine (Figure 4b) to form conjugates (*m/z* 517 and *m/z* 373, respectively) via the thiol group. General structures for probable GSH and NAC conjugates of 2-OH-AC are shown in Figure 8. We suspect that 2-OH-AC is likely to undergo a P450-catalyzed oxidative dehydrogenation which results in the formation of a reactive intermediate in the form of a quinone imine (Guengerich 2007), as, *e.g.*, it takes place in a metabolic pathway of the acetaminophen (Jollow *et al.* 1973; Larson 2007). For this mechanism, a quinone imine of 2-OH-AC has to be the precursor of the adduct as the corresponding quinone imine would have the *m/z* ratio of 210 in the positive-ion mode detection. However, this intermediate product, presumably due to its short life span and high reactivity, was not directly detected in the mass voltammogram of pure 2-OH-AC. It is important to note that the same type of GSH S-conjugate was detected after *in vitro* liver microsomal incubations in an NADPH-dependent manner and in the reaction mixture from the electrolysis experiment (Figure 6). Quinone

imines are well known reactive intermediates which very often undergo adduct formation with crucial cellular compounds such as GSH, structural proteins, enzymes and/or DNA (Bolton *et al.* 2000; Zhou *et al.* 2005). As a consequence, these compounds can cause a variety of hazardous effects *in vivo*, including acute cytotoxicity, immunotoxicity, and carcinogenesis, especially in the case of depleted levels of cellular GSH (Lohmann *et al.* 2010). However, the fact that reactive metabolite of 2-OH-AC may exist and, as it has been shown, may undergo adduct formation does not consequently imply that it causes toxicity (Evans *et al.* 2004) so further studies are needed to elucidate whether this metabolite contributes to the 2-OH-AC toxicity *in vivo*.

The results of our studies clearly prove that EC-based approach has the potential to simulate the majority of oxidative metabolism reaction, including the simulation of reactive metabolite formation and its binding to biomolecules (*e.g.*, GSH). The observed dehydrogenation, hydroxylation and oxidation of acridinone molecule are in general agreement with reports on the types of P450-catalyzed reactions being simulated by electrochemistry (Lohmann & Karst 2008; Lohmann *et al.* 2010). Our observations on product structures may be advantageous from the viewpoint of the structural factors that influence the reactivity and functional group interactions of the compound, providing a good approximation of what may occur *in vivo*.

Conclusions

The present study demonstrated the significance of electrochemistry coupled on-line with mass spectrometry in drug metabolism studies. This combination appeared to be a suitable tool for a simulation of some types of oxidative drug metabolic reactions related to cytochromes P450, and for studying the formation of reactive metabolites. In this investigation, 2-hydroxyacridinone (2-OH-AC), the reference compound for antitumor-active imidazo- and triazoloacridinone derivatives, was easily oxidized in an electrochemical thin-layer cell to several different products. To trap potentially reactive metabolite(s) two types of nucleophilic trapping agents, reduced GSH and NAC, both with nucleophilic thiol group, were used. This allowed us to identify and characterize a novel GSH (NAC) S-conjugate of 2-OH-AC. The postulated reactive quinone imine metabolite of 2-OH-AC may potentially be involved in a number of biochemical transformations, and can be responsible for the antitumor activity of acridinone derivatives. The role of this reactive metabolite requires further investigation.

The electrochemical method we proposed here represented a good alternative for classical metabolic studies with the principal advantage which is the absence of proteins in the reaction medium. It will be very useful in further studies on metabolic transformations of antitumor imidazo- and triazoloacridinone drugs. Considering pharmacological aspect, our findings may provide important guidelines for the further modification of the acridinone compounds so they contribute to the design and the development of safer and more effective therapeutic agents.

Acknowledgments

This work was supported by the National Science Center (Poland) under Grant number 2012/07/D/NZ7/03395..

Declaration of interest statement

The authors confirm that this article content has no conflicts of interest.

References

Acheson RM. (1973). Acridines. In: Acheson RM, ed. The chemistry of heterocyclic compounds. New York, Interscience Publishers, Inc., p. 141.

Augustin E, Mość-Rompa A, Skwarska A, Witkowski JM, Konopa J. (2006). Induction of G2/M phase arrest and apoptosis of human leukemia cells by potent antitumor triazoloacridinone C-1305. Biochem Pharmacol 72: 1668-1679.

Baillie TA, Cayen MN, Fouda H, Gerson RJ, Green JD, Grossman SJ, *et al.* (2002). Drug metabolites in safety testing. Toxicol Appl Pharmacol 182: 188-196.

Baumann A, Lohmann W, Rose T, Ahn KC, Hammock BD, Karst U, *et al*. (2010). Electrochemistry-mass spectrometry unveils the formation of reactive triclocarban metabolites. Drug Metab Dispos 38: 2130-2138.

Bolton JL, Trush MA, Penning TM, Dryhurst G, Monks TJ. (2000). Role of quinones in toxicology. Chem Res Toxicol 13: 135-160.

Brandon EF, Raap CD, Meijerman I, Beijnen JH, Schellens JH. (2003). An update on in vitro test methods in human hepatic drug biotransformation research: pros and cons. Toxicol Appl Pharmacol 189: 233-246.

Bussy U, Boisseau R, Thobie-Gautier C, Boujtita M. (2015). Electrochemistry-mass spectrometry to study reactive drug metabolites and CYP450 simulations. Trends Anal Chem 70: 67-73.

Bussy U, Boujtita M. (2014). Advances in the electrochemical simulation of oxidation reactions mediated by cytochrome P450. Chem Res Toxicol 27: 1652-1668.

Cholody WM, Horowska B, Paradziej-Lukowicz J, Martelli S, Konopa J. 1996. Structure-activity relationship for antineoplastic imidazoacridinones: synthesis and antileukemic activity in vivo. J Med Chem 39: 1028-1032.

Cholody WM, Martelli S, Konopa J. (1990). 8-Substitued 5-[(aminoalkyl)amino]-6H-v-triazolo[4,5,1-de]acridin-6-ones as potential antineoplastic agents. Synthesis and biological activity. J Med Chem 33: 2852-2856.

Cholody WM, Martelli S, Lukowicz J, Konopa J. (1990). 5-[(Aminoalkyl)amino]imidazo[4,5,1-de]acridin-6-ones as a novel class of antineoplastic agents. Synthesis and biological activity. J Med Chem 33: 49-52.

Dziegielewski J, Konopa J. (1996). Interstrand crosslinking of DNA induced in tumor cells by a new group of antitumor imidazoacridinones. Proc Am Assoc Cancer Res 37: 410.

Dziegielewski J, Konopa J. (1998). Characterisation of covalent binding to DNA of antitumor imidazoacridinone C-1311, after metabolic activation. Ann Oncol Suppl 1: 137.

Dziegielewski J, Slusarski B, Konitz A, Skladanowski A, Konopa J. (2002). Intercalation of imidazoacridinones to DNA and its relevance to cytotoxic and antitumor activity. Biochem Pharmacol 63: 1653-1662.

Evans DC, Watt AP, Nicoll-Griffith DA, Baillie TA. (2004). Drug-protein adducts: An industry perspective on minimizing the potential for drug bioactivation in drug discovery and development. Chem Res Toxicol 17: 3-16.

Faber H, Jahn S, Kunnemeyer J, Simon H, Melles D, Vogel M, *et al.* (2011). Electrochemistry/liquid chromatography/mass spectrometry as a tool in metabolism studies. Angew Chem 50: A52-58.

Guengerich FP. (2007). Oxidative, reductive and hydrolytic metabolism of drugs. In: Zhang D, Zhu M, Humphreys WG, eds. Drug metabolism in drug design and development. New York, John Willey & Sons, Inc., p. 265.

Harding MM, Grummitt AR. (2003). 9-hydroxyellipticine and derivatives as chemotherapy agents. Mini Rev Med Chem 3: 67-76.

Inoue K, Fukuda K, Yoshimura T, Kusano K. (2015). Comparison of the reactivity of trapping reagents toward electrophiles: cysteine derivatives can be bifunctional trapping reagents. Chem Res Toxicol 28: 1546-1555.

Jennings GS, Strauss M. (1999). Immortalization of hepatocytes through targeted deregulation of the cell cycle. In: Al-Rubeai M, ed. Cell engineering. the Netherlands, Kluwer Academic Publishers, p. 259.

Jollow DJ, Mitchell JR, Potter WZ, Davis DC, Gillette JR, Brodie BB. (1973). Acetaminophen-induced hepatic necrosis. II. Role of covalent binding in vivo. J Pharmacol Exp Ther 187: 195-202.

Jurva U, Wikstrom HV, Weidolf L, Bruins AP. (2003). Comparison between electrochemistry/mass spectrometry and cytochrome P450 catalyzed oxidation reactions. Rapid Commun Mass Spectrom 17: 800-810.

Kalgutkar AS, Soglia JR. (2005). Minimising the potential for metabolic activation in drug discovery. Expert Opin Drug Metab Toxicol 1: 91-142.

Koba M, Konopa J. (2007). Interactions of antitumor triazoloacridinones with DNA,. Acta Biochim Pol 54: 297-306.

Kusnierczyk H, Cholody WM, Paradziej-Lukowicz J, Radzikowski C, Konopa J. (1994). Experimental antitumor activity and toxicity of the selected triazolo- and imidazoacridinones. Arch Immunol Ther Exper (Warsz) 42: 415-423.

Larson AM. (2007). Acetaminophen hepatotoxicity. Clin Liver Dis 11: 525-548.

Lemke K, Wojciechowski M, Laine W, Bailly C, Colson P, Baginski M, *et al.* (2005). Induction of unique structural changes in guanine-rich DNA regions by the triazoloacridone C-1305, a topoisomerase II inhibitor with antitumor activities. Nucleic Acids Res 33: 6034-6047.

Lohmann W, Karst U. (2008). Biomimetic modeling of oxidative drug metabolism: strategies, advantages and limitations. Anal Bioanal Chem 391: 79-96.

Lohmann W, Baumann A, Karst U. (2010). Electrochemistry and LC-MS for metabolite generation and identification: tools, technologies and trends. LC•GC Europe January: 1-7.

Marks TA, Venditti JM. (1976). Potentiation of actinomycin D or adriamycin antitumor activity with DNA. Cancer Research 36: 496-504.

Martignoni M, Groothuis GM, de Kanter R. (2006). Species differences between mouse, rat, dog, monkey and human CYP-mediated drug metabolism, inhibition and induction. Expert Opin Drug Metab Toxicol 2: 875-894.

Mazerska Z, Dziegielewski J, Konopa J. (2001). Enzymatic activation of a new antitumour drug 5-diethylaminoethylamino-8-hydroxyimidazo-acridinine, C-1311, observed after its intercalation into DNA. Biochem Pharmacol 61: 685-694.

Mazerska Z, Zamponi S, Marassi R, Martelli S, Konopa J. (1997). Electrochemical oxidation of antitumor imidazoacridinone derivatives and the reference 2-hydroxyacridinone. J. Electroanal Chem 427: 71-78.

Mazerska Z, Zamponi S, Marassi R, Sowinski P, Konopa J. (2002). The products of electro- and photochemical oxidation of 2-hydroxyacridinone, the reference compound of antitumor imidazoacridinone derivatives. J Electroanal Chem 521: 144-154.

Nouri-Nigjeh E, Bischoff R, Bruins AP, Permentier HP. (2011). Electrochemistry in the mimicry of oxidative drug metabolism by cytochrome P450s. Curr Drug Metab 12: 359-371.

Orhan H, Vermeulen NPE. (2011). Conventional and novel approaches in generating and characterization of reactive intermediates from drugs/drug candidates. Curr Drug Metab 12: 383-394.

Park BK, Boobis A, Clarke S, Goldring CE, Jones D, Kenna JG, *et al.* (2011). Managing the challenge of chemically reactive metabolites in drug development. Nat Rev Drug Discov 10: 292-306.

Permentier HP, Bruins AP, Bischoff R. (2008). Electrochemistry-mass spectrometry in drug metabolism and protein research. Mini Rev Med Chem 8: 45-56.

Pinto N, Dolan ME. (2011). Clinically relevant genetic variations in drug metabolizing enzymes. Curr Drug Metab 12: 487-497.

Prakash C, Sharma R, Gleave M, Nedderman A. (2008). In vitro screening techniques for reactive metabolites for minimizing bioactivation potential in drug discovery. Curr Drug Metab 9: 952-964.

Sichilongo KF, Famuyiwa SO, R. Kibechu R. (2011). Pre-electrospray ionisation manifold methylation and post-electrospray ionisation manifold cleavage/ion cluster formation observed during electrospray ionisation of chloramphenicol in solutions of methanol and acetonitrile for liquid chromatography-mass spectrometry employing a commercial quadrupole ion trap mass analyser. Eur J Mass Spectrom (Chichester) 17: 255-264.

Skladanowski A, Plisov SY, Konopa J, Larsen AK. (1996). Inhibition of DNA topoisomerase II by imidazoacridinones, new antineoplastic agents with strong activity against solid tumors. Mol Pharmacol 49: 772-780.

Srivastava A, Maggs JL, Antoine DJ, Williams DP, Smith DA, Park BK. (2010). Role of reactive metabolites in drug-induced hepatotoxicity. Handb Exp Pharmacol 196 (2010) 165-194.

Volk KJ, Yost RA, Brajter-Toth A. (1992). Electrochemistry on line with mass spectrometry insight into biological redox reactions. Anal Chem 64: 21A-26A.

Wang L, Chai Y, Tu P, Sun C, Pan Y. (2011). Formation of [M + 15](+) ions from aromatic aldehydes by use of methanol: in-source aldolization reaction in electrospray ionization mass spectrometry. J Mass Spectrom 46: 1203-1210.

Zanger UM, Schwab M. (2013). Cytochrome P450 enzymes in drug metabolism: Regulation of gene expression, enzyme activities, and impact of genetic variation. Pharmacol Therapeut 138: 103-141.

Zhou S, Chan E, Duan W, Huang M, Chen YZ. (2005). Drug bioactivation, covalent binding to target proteins and toxicity relevance. Drug Metab Rev 37: 41-213.

Tables with captions

Table 1

EC and ESI-Q-TOF-MS(/MS) parameters as applied in direct EC/MS(/MS) and in MS(/MS) experiments for determination of accurate masses of product ions and getting ion fragmentation.

	Parameter	Value or setting
EC settings	Flow rate	30 µL·min^{-1}
	Potential	0 – 2.5 V (10 mV steps)
	EC operating mode	scan
	Cycle	continuous
MS(/MS) settings	The range of *m/z*	100 – 600
	Ion source	dual ESI
	Ion polarity	positive
	MS operating mode	scan
	Capillary voltage	3500 V
	Nebulizer gas (N_2) pressure	35 psig
	Drying gas (N_2) flow	10 L·min^{-1}
	Drying gas temperature	325 °C
	Fragmentor	175 V
	Skimmer	45 V
	OCT 1 RF Vpp	750 V
	Rate	1,5 spectra·s^{-1}
	MS/MS method - Slope - Offset	targeted - 4 *m/z* - 5 V

Table 2

A summary of molecular formulas of 2-OH-AC and its products found after electrochemical oxidation on a GC working electrode in a potential range of 0 – 2.5 V versus Pd/H_2. Base

Product	Measured *m/z* / Da	Calculated *m/z* / Da [a]	Deviation / ppm	Molecular formula of $[M+H]^+$ ion	MS/MS fragment ions	Predicted modification of 2-OH-AC molecule
2-OH-AC	212.0712	212.0706	2.9	$C_{13}H_{10}NO_2$	-	-
P1a, b	226.0501	226.0499	1.1	$C_{13}H_8NO_3$	212	- 2H + O
P2	227.0578	227.0577	0.5	$C_{13}H_9NO_3$	212	- H + O
P3	228.0648	228.0655	-3.1	$C_{13}H_{10}NO_3$	212, 226, **227**	+ O
P4	240.0658	240.0655	1.2	$C_{14}H_{10}NO_3$	212, **227**, 228	+ CO
P5	242.0818	242.0812	2.6	$C_{14}H_{12}NO_3$	212, **228**, 240	+ 2H + CO
P6	256.0614	256.0604	3.8	$C_{14}H_{10}NO_4$	212, 226, **228**, 240, 242	+ CO_2
P7	258.0758	258.0761	-1.2	$C_{14}H_{12}NO_4$	212, 226, **228**, 240, 242, 256	+ 2H + CO_2
P8	421.1176	421.1183	-1.6	$C_{26}H_{17}N_2O_4$	212	2-OH-AC dimer

fragment ions are shown in bold.

[a] Calculated using Molecular Mass Calculator freeware version v2.02.

Table 3

A summary of neutral losses and fragmentations for ions attributed to the respective glutathione S-conjugate of the 2-OH-AC.

MS/MS collision-induced dissociation of glutathione S-conjugate			2-OH-AC		
			Measured *m/z* / Da	Calculated *m/z* / Da [a]	Deviation / ppm
Neutral losses	Parent	*m/z* / Da	517.1382	517.1387	1.04
	Glycine	75.0320	None	442.1067	None
	Anhydroglutamic acid	129.0426	388.0963	388.0962	-0.39
	Glutamine	146.0691	None	371.0696	None
	γ-Glu-Ala-Gly	275.1117	244.0421 [b]	244.0427	2.34
	Glutathione (S-oxide)	322.0709	None	195.0679	None

[a] Calculated using Molecular Mass Calculator freeware version v2.02.
[b] Neutral loss of γ-Glu-Ala-Gly + 2H.

Figure captions

Figure 1

Instrumental set-ups used for (**a**) the electrochemical simulation of the oxidative metabolism of 2-OH-AC and (**b**) the investigation of the reactivity of 2-OH-AC oxidation products towards GSH (NAC).

Legend: 1 – infusion syringe pump, 2 – potentiostat, 3 – electrochemical thin-layer cell (EC) – reactor cell, 4 – mass spectrometer (MS), 5 – T-piece and 100 µL mixing coil

Chemical structures of the investigated 2-hydroxyacridinone (2-OH-AC) compound and glutathione (GSH)/*N*-acetylcysteine (NAC)**,** used as nucleophilic trapping agents, are presented in the frame.

Figure 2

Cyclic voltammograms of 0.5 mM 2-OH-AC (**a**) alone and (**b**) in the mixture with 5 mM GSH in 0.02 M PBS buffer, pH 7.40, versus electrolysis progress. Experimental conditions: potential range -0.2 – 1.2 V; scan rate 100 $mV \cdot s^{-1}$; T = 21 ^{o}C; ϕ GC 3 mm.

Figure 3

Two-dimensional plot (2-D mass voltammogram) of 10 µM 2-OH-AC oxidation at a GC working electrode (extracted ion intensity versus the progress of the electrochemical oxidation; positive-ion mode). The *m/z* ratios shown correspond to the protonated 2-OH-AC and its products (see legend). Experimental conditions: potential range 0 – 2.5 V; scan rate 10 $mV \cdot s^{-1}$, continuous; T = 21 ^{o}C; ϕ GC 8 mm. The insets show the representative mass spectrum of 2-OH-AC without voltage applied to the electrochemical cell (cell off; top left corner) and after electrochemical oxidation (cell on; top right corner).

Figure 4

Two-dimensional plots (2-D mass voltammograms) of 10 µM 2-OH-AC oxidation at a GC working electrode in the presence of 100 µM (a) GSH and (b) NAC (extracted ion intensity versus the progress of the electrochemical oxidation; positive-ion mode). The *m/z* ratios shown correspond to the protonated 2-OH-AC and GSH or NAC S-conjugate (see legend).

Experimental conditions: potential range 0 – 2.5 V; scan rate 10 $mV \cdot s^{-1}$, continuous; T = 21 ^{o}C; ϕ GC 8 mm.

Figure 5

The representative mass spectrum of a mixture of 2-OH-AC and GSH (**a**) without voltage applied to the electrochemical cell (cell off) and (**b**) after electrochemical oxidation (cell on). The insets show a zoom in the mass range from *m/z* 510 to 520 (positive-ion mode). (**c**) Fragmentation spectrum of the conjugation product *m/z* 517.

Figure 6

(**a**) The representative high performance LC chromatograms of the reaction mixtures obtained after metabolism simulation of 0.5 mM 2-OH-AC in the absence (black line) and the presence (grey dashed line) of 5 mM GSH in RLM incubations (enzymatic oxidation) and from controlled-potential electrolysis (oxidation by CPE). The inset shows UV-Vis spectra of GSH S-conjugate and 2-OH-AC. (**b**) The representative extracted ion chromatograms for 2-OH-AC oxidation in electrochemical cell.

Figure 7

Proposed oxidation reaction pathways of 2-OH-AC observed in the electrochemical cell. Tentative structures were derived on the basis of accurate mass measurements and MS/MS fragmentation patterns. Probable isomeric compounds are gathered in encircled blocks.

Figure 8

Schematic representation of the proposed mechanism of the 2-OH-AC electrochemical oxidation and GSH (NAC) S-conjugate formation.

Title:

Phase I and phase II metabolism simulation of antitumor-active 2-hydroxyacridinone with electrochemistry coupled on-line with mass spectrometry.

Abstract

1. Here, we report the metabolic profile and the results of associated metabolic studies of 2-hydroxyacridinone (2-OH-AC), the reference compound for antitumor-active imidazo- and triazoloacridinones.
2. Electrochemistry coupled with mass spectrometry was applied to simulate the general oxidative metabolism of 2-OH-AC for the first time. The reactivity of 2-OH-AC products to biomolecules was also examined. The usefulness of the electrochemistry for studying the reactive drug metabolite trapping (conjugation reactions) was evaluated by the comparison with conventional electrochemical (controlled-potential electrolysis) and enzymatic (microsomal incubation) approaches.
3. 2-OH-AC oxidation products were generated in an electrochemical thin-layer cell. Their tentative structures were assigned based on tandem mass spectrometry in combination with accurate mass measurements. Moreover, the electrochemical conversion of 2-OH-AC in the presence of reduced glutathione and/or *N*-acetylcysteine unveiled the formation of reactive metabolite-nucleophilic trapping agent conjugates (*m/z* 517 and *m/z* 373, respectively) via the thiol group. This glutathione S-conjugate was also identified after electrolysis experiment as well as was detected in liver microsomes.
4. Summing up, the present work illustrates that the electrochemical simulation of metabolic reactions successfully supports the results of classical electrochemical and enzymatic studies. Therefore, it can be a useful tool for synthesis of drug metabolites, including reactive metabolites.

Keywords:

in vitro metabolism; metabolic activation; electrochemical oxidation; electrochemistry-mass spectrometry; metabolite electrosynthesis; reactive metabolite; glutathione S-conjugate;

Introduction

Solid understanding of the metabolic pathways and the biotransformation mechanisms of new drug candidates is a crucial point in the drug discovery and development processes. Overall, it allows to elucidate the metabolic activation as well as the deactivation routes of new biologically active compounds, especially in respect to their possible toxicity (Park *et al.* 2011). The identification of metabolites helps to eliminate the inappropriate candidates at an early stage, before the more expensive development phases will be performed (Bussy & Boujtita 2014). Particularly, it is very important that the formation of chemically reactive intermediates is checked (Baillie *et al.* 2002), because an increasing number of reports indicate that they are responsible for the majority of rapid and unexpected drug toxic effects (Kalgutkar & Soglia 2005; Srivastava *et al.* 2010; Orhan & Vermeulen 2011). The relationship between drug metabolism and adverse drug reactions was first demonstrated with the analgesic agent acetaminophen (Jollow *et al.* 1973; Larson 2007). Reactive intermediates, generated usually via cytochrome P450 (P450)-catalyzed oxidative reactions, have the potential for covalent binding to cellular nucleophiles such as purine and pyrimidine bases of DNA or thiols of proteins, and form stable adducts. Adduct formation may alter biological functions of these biomolecules what ultimately leads to a toxic response (Brandon *et al.* 2003).

Metabolic activation of new drugs to reactive intermediates is currently assessed in the presence or the absence of reactive endogenous nucleophiles, such as reduced glutathione (GSH), *N*-acetylcysteine (NAC) or β-lactoglobulin A (βLGA), a model protein. In practise, the reaction usually involves the *in vitro* incubation of a studied compound with an excess of the selected chemical-trapping agent in hepatocytes or liver microsomes (as a source of cytochrome P450 isoenzymes). *In vivo* experiments involve laboratory animals (Kalgutkar & Soglia 2005). However, performing these biological schemes is usually laborious and time-consuming. Despite continuous improvements in metabolite-identification tools, the identification of some reactive metabolites remains difficult due to the matrix complexity, low concentration or their binding to matrix bio-components (Bussy *et al.* 2015). Isolated

hepatocytes have only a very limited proliferative potential *in vitro* and a correspondingly short life-span in primary culture. Their fenotype is unstable and the level and activities of enzymes, such as cytochromes P450, fall quickly in a few days (Jennings & Strauss 1999). Also liver microsomes offer a limited reproducibility. Additionally, because of genetic polymorphisms, variations in the gene expression for individual drug-metabolising izoenzymes in each organism have to be taken into account (Pinto & Dolan 2011; Zanger & Schwab 2013).

As an alternative to the existing methods for studies on drug metabolism and toxicity, the electrochemical simulation of P450-catalyzed phase I reactions, mostly initiated by a single-electron transfer, has been developed (Volk *et al.* 1992; Lohmann & Karst 2008; Faber *et al.* 2011). Overall, it allows to simulate a wide variety of oxidation-reduction (redox) processes occurring in living organisms (Jurva *et al.* 2003; Nouri-Nigjeh *et al.* 2011). The combination of electrochemistry (EC) coupled on-line with mass spectrometry (MS) creates a powerful platform for rapid generation (in the electrochemical cell) and detection (by mass spectrometry) of a series of metabolic products, including observation of reactive metabolites (Permentier *et al.* 2008; Faber *et al.* 2011; Bussy & Boujtita 2014). Use of EC/MS improves the conventional methods of drug metabolism studies. It is a purely instrumental technique with a simple set-up that enables the generation of drug metabolites in the absence of biological matrices in the reaction medium. So, the application of EC/MS helps to overcome many of the laborious tasks related to isolation and identification of metabolic products formed *in vitro* (cultured hepatocytes, liver microsomes, purified enzymes) or *in vivo* (urine, plasma, *etc.*) (Orhan & Vermeulen 2011; Faber *et al.* 2011). Moreover, on-line combining EC with MS can provide valuable information about metabolically labile sites in a drug molecule and predict its reliable metabolic profile in a much shorter time (Jurva *et al.* 2003; Permentier *et al.* 2008).

Recently extensive research have been conducted in our group to determine the possible metabolic pathways of potential antitumor drugs and their model compounds. The objective of the investigations presented here was to develop and evaluate an on-line EC/MS method

for the simulation of oxidative metabolism of 2-hydroxyacridinone (2-OH-AC) (a structure in the frame in Figure 1), a simple reference compound for high antitumor-active imidazo- and triazoloacridinones.

The preliminary studies in this field were performed earlier by the application of cyclic voltammetry, spectroelectrochemical measurements, and controlled-potential electrolysis (Mazerska *et al.* 1997, 2002). These experiments indicated the ability of 2-OH-AC to undergo oxidative metabolic activation in the living organism. However, no data for acridinone derivatives are yet available using the direct coupling EC with MS. The studies presented here were undertaken with respect to the usefulness of EC/MS technique for futher investigation on the oxidative metabolic activation and the identification of potential reactive metabolites formed during the metabolism of antitumor-active imidazoacridinone C-1311 and triazoloacridinone C-1305. These compounds, developed in our laboratory, have demonstrated significant cytotoxic and antitumor activities (Cholody *et al.* 1990, 1996; Kusnierczyk *et al.* 1994). The data obtained so far indicate that they have different spectrum of antitumor activity and exhibit various mechanisms of action at the molecular level (Dziegielewski & Konopa 1996; Skladanowski *et al.* 1996; Dziegielewski *et al.* 2002; Lemke *et al.* 2005; Augustin *et al.* 2006). Metabolic activation is the leading concept for the reason how imidazo- and triazoloacridinone derivatives cause high antitumor effect (Dziegielewski & Konopa 1998; Mazerska *et al.* 2001; Koba & Konopa 2007). It is assumed that the hydroxyl group in the acridinone ring provides the susceptibility of these compounds to oxidative metabolism. The formation of the intermediate, characterized as a quinone imine structure, that expresses antitumor activity, has been shown, for example, in the case of 9-hydroxyellipticine (Harding & Grummitt 2003). A known quinone imine with activity against human tumor cells is actinomycin D (Marks & Venditti 1976).

In this work, the ability of EC/MS to expedite the generation and identification of the main phase I metabolites of 2-OH-AC will be discussed. The formation of the reactive 2-OH-AC intermediate metabolite and the possibility to simulate its covalent binding to biomolecule (*i.e.*, glutathione (GSH) and/or *N*-acetylcysteine (NAC) as biomarkers of metabolic activity;

phase II metabolism) are also taken into account. Furthermore, to show the capability of electrochemistry to simulate certain P450-mediated reactions, the results obtained by EC were also compared with those gained after controlled-potential electrolysis (CPE) and conventional *in vitro* studies by conducting incubations of 2-OH-AC with human and rat liver microsomes (HLMs and RLMs, respectively). The products of electrolysis and enzymatic transformations of 2-OH-AC were analysed by reversed-phase liquid chromatography (LC) with UV-Vis detection and/or diode array detection, and monitored by MS. The relation between the products generated electrochemically and enzymatically for the model compound 2-OH-AC can provide a clue to the nature of their metabolic pathway initiation (Volk *et al.* 1992). It opens up further perspectives directed to the search for more effective and less toxic antitumor drugs among acridinone derivatives. It is significant because improves the risk evaluation for potential drugs in the optimal chemotherapy schedules designed for individual patients.

List of abbreviations:

CPE, controlled-potential electrolysis;

CV, cyclic voltammetry, cyclic voltammogram;

EC, electrochemistry, electrochemical cell;

ESI, electrospray ionization;

GC, glassy carbon;

GSH, glutathione (reduced form);

HLMs, human liver microsomes;

2-OH-AC, 2-hydroxyacridinone;

m/z, mass-to-charge ratio;

MS, mass spectrometry, mass spectrometer;

MS/MS, tandem mass spectrometry;

NADPH, β-nicotinamide adenine dinucleotide 2'-phosphate tetrasodium salt (reduced form);

NAC, *N*-acetylcysteine;

P450, cytochrome P450;

PBS, phosphate-buffered saline;

Q-TOF, quadrupole-time of flight;

RLMs, rat liver microsomes;

LC, liquid chromatography;

Parts of this work were presented at the 13th European ISSX Meeting (Glasgow, Scotland, 2015) and at the 2nd Congress BIO 2016 (Wrocław, Poland, 2016).

Materials and methods

Chemicals and enzymes

An acridinone derivative, a 2-hydroxyacridinone (2-OH-AC) was synthesized in our laboratory according to the method described earlier (Acheson 1973). The following chemicals were purchased from Sigma-Aldrich (St. Louis, MO, USA): *N*-acetylcysteine (NAC), dipotassium phosphate (K_2HPO_4), disodium phosphate (Na_2HPO_4), formic acid (HCOOH), L-glutathione reduced (GSH), monopotassium phosphate (KH_2PO_4), monosodium phosphate (NaH_2PO_4), and semicarbazide hydrochloride. Methanol (gradient grade for liquid chromatography) and *β*-nicotinamide adenine dinucleotide 2'-phosphate tetrasodium salt (*β*-NADPH) were obtained from Merck KGaA (Darmstadt, Germany). Ammonium formate ($HCOONH_4$) was ordered from Fisher Scientific (Loughborough, UK). Aluminum oxide (Al_2O_3) powder in form of 1-µm alumina suspension, for polishing of electrodes, was delivered by TESTING Sp z o.o. (Katowice, Poland). All other commercially available chemicals and reagents were of the highest possible grade available. Ultrapure water (0.056 $\mu S \cdot cm^{-1}$), used in all the experiments, was passed through a Milli-Q water purification system from Merck KGaA (Darmstadt, Germany) or water distillation system from Hydrolab Sp. z o.o. sp.k. (Straszyn, Poland).

Pooled human liver microsomes (HLMs), mixed gender, from 50 donors (protein concentration, 20 $mg \cdot mL^{-1}$; P450 content, 411 $pmol \cdot mg^{-1}$ protein) and pooled rat liver microsomes (RLMs) from untreated, male Sprague-Dawley rats (protein concentration, 20 $mg \cdot mL^{-1}$; P450 content, 680 $pmol \cdot mg^{-1}$ protein) were purchased from Tebu-bio (Le Perray-En-Yvelines, France).

General instrumentation

Electrochemical measurements

Electrochemical measurements of the oxidation-reduction properties of 2-OH-AC were performed with controlled-potential electrolysis (CPE) and by electrochemical metabolism simulation in a three-electrode thin-layer cell (EC).

CPE was performed using an Autolab (Eco Chemie B.V., Utrecht, The Netherlands), model PGSTAT 12 potentiostat, controlled via producer's software. The three-electrode system, consisting of a cylinder glassy carbon (GC) working electrode (ϕ = 3 mm and 13 mm long; A = 1.296 cm^2), an Ag/AgCl/3 M KCl reference electrode and a platinum-wire counter electrode, were employed. During chronoamperometric measurements the working electrode as well as the analyzed solution were placed in a glass tube closed with a "Vicor" plug to separate the electrolyzed solution from the main solution.

Simulation of the oxidative metabolism reactions of 2-OH-AC was accomplished in an electrochemical thin-layer cell equipped with a disc glassy carbon (GC) working electrode (ϕ = 8 mm; A = 0.502 cm^2) and a Pd/H_2 reference electrode (reactor cell; Antec Leyden, Zoeterwoude, The Netherlands). Carbon-loaded PTFE (polytetrafluoroethylene) served as auxiliary electrode. The cell potentials were applied using a ROXY EC System (Antec Leyden) controlled by Antec Dialogue software (Antec Leyden). The outlet of the electrochemical cell was connected directly to an electrospray ionization (ESI) source of a quadrupole-time of flight (Q-TOF) mass spectrometer (Agilent Technologies, Santa Clara, CA, USA) (Figure 1a). S-Conjugate formation of 2-OH-AC and GSH (NAC) was established using a T-piece and a 100 µL mixing coil placed between reactor cell and the ESI source (Figure 1b). The relevant EC conditions can be viewed in Table 1.

Liquid chromatographic analyses

For all analyses of 2-OH-AC, liquid chromatographic (LC) separations were performed on a reversed-phase 5-µm Suplex pKb-100 analytical column (4.6 mm x 250 mm, C18) (Supelco Inc., Bellefonte, PA, USA) with Waters Associates HPLC system (Waters Co., Milford, MA, USA). It was equipped with a model 600E system controller, a model 7725i Rheodyne injector, and a model 2996 photodiode array detector (DAD) controlled with Millennium software (Waters Co.). The LC analyses were carried out at a flow rate of 1 $mL \cdot min^{-1}$ with the following mobile phase system: a linear gradient from 15% to 80% methanol in 0.05 M aqueous ammonium formate buffer (pH 3.40 adjusted with formic acid)

for 25 min, followed by a linear gradient from 80% to 100% methanol in ammonium formate buffer, pH 3.40, for 3 min. The eluates were monitored at 380 nm.

Mass spectrometry

Mass spectrometric detection, identification, and fragmentation of 2-OH-AC products were carried out in the positive-ion mode by recording full scan spectra (*m/z* 100 – 600). To ensure accurate mass during the experiment, the mass spectrometer was calibrated on a daily basis, prior to sample analysis. The corresponding conditions for the ESI-Q-TOF-MS(/MS) measurements are listed in Table 1.

Controlled-potential electrolysis of 2-OH-AC

The controlled-potential electrolysis was performed in 0.02 M phosphate-buffered saline (PBS), pH 7.40, obtained by mixing Na_2HPO_4 and KH_2PO_4, and adding the appropriate amounts of NaCl and KCl to reach their concentrations of 0.15 and 0.002 M, respectively. Each time before the electrolysis experiments the GC working electrode was briefly polished with 1-μm Al_2O_3 powder on a wet pad. After polishing step, to remove alumina completely from the surface, the electrode was rinsed with a direct stream of ultrapure water. To eliminate the electric noise the electrochemical cell was placed in a Faraday cage. The chronoamperometric experiments of 0.5 mM 2-OH-AC in the absence and the presence of 10-fold excess of GSH were performed at 0.50 V. The electrolysis progress was monitored by voltammetric, spectroscopic, chromatographic, and spectrometric methods. The experiments have been performed at room temperature (21 ºC).

Electrochemical simulation of the oxidative metabolism of 2-OH-AC

For the electrochemical conversion, a 10-μM 2-OH-AC solution in electrolyte (0.1% formic acid in water/methanol, 50/50, *v/v*) was pumped (SP2 – ROXY dual piston syringe pump; Antec Leyden) through the electrochemical cell at a constant flow rate of 30 $\mu L \cdot min^{-1}$. The potential of working electrode in the reactor cell was ramped between 0 and 2500 mV (scan rate 10 $mV \cdot s^{-1}$). The outlet of the reactor cell was connected on-line to the ESI-MS source (Figure 1a). To identify potential aldehyde products the oxidized sample was collected in a vial containing semicarbazide (dissolved in ultrapure water) to give a final

concentration of 5 mM. After collection, the samples from the trapping experiments were kept at 25 ºC for 1 h before analysis by LC/MS.

The properties of the sample solvent may influence the conversion efficiency in the electrochemical cell. Therefore, the electrochemical simulation of the oxidative metabolism of 2-OH-AC has been also performed in two different electrolyte solutions containing acetonitrile (0.1% formic acid or 20 mM ammonium formate (pH 3.40), respectively, in water/acetonitrile, 50/50, *v/v*).

On-line trapping of oxidation product with glutathione (N-acetylcysteine)

To identify possible S-conjugate(s) with GSH (NAC), the EC/MS set-up described above was slightly modified (Figure 1b). A 10-µM 2-OH-AC solution in electrolyte was pumped through the electrochemical cell at a constant flow rate of 30 µL·min^{-1}. 100 µM GSH (NAC) in ultrapure water was added at the same flow rate to the effluent of the electrochemical cell via a T-piece into a 100 µL mixing coil. The effluent from the mixing coil was injected directly into the ESI-MS interface.

In vitro microsomal incubations

Human or rat liver microsomal incubations (1 mg·mL^{-1} protein) were performed with 50 µM 2-OH-AC, 1 mM NADPH, and 1 mM GSH in a potassium phosphate-buffered solution (0.1 M, pH 7.40) at 37 °C for 1 h, in a total volume of 100 µL. The incubations were terminated by adding ice-cold methanol to the incubation mixtures (50:50, *v/v*). The samples were then vortexed, placed in ice for 10 min, and centrifuged at 10000 x g for 10 min. Aliquots of the supernatants (150 µL) were then analyzed directly by reversed-phase LC with UV-Vis detection and/or diode array and multiple wavelength detection, and monitored by MS. The three types of control incubations were applied, the first without test compound, the second without NADPH, and the third without GSH.

Results

In order to provide an important insight into the mechanism of antitumor action of imidazo- and triazoloacridinones, the electrochemical oxidation of their simpler reference compound,

2-OH-AC, was investigated. The ability of 2-OH-AC to undergo oxidative metabolic activation was studied by applying the direct combination of electrochemistry and mass spectrometry (EC/MS). For 2-OH-AC no EC/MS data were found before. Electrochemical conversion of 2-OH-AC was conducted in parallel to controlled-potential electrolysis (CPE) and *in vitro* experiments using liver microsomes.

Controlled-potential electrolysis of 2-OH-AC

At first, cyclic voltammetry (CV) was used to initially investigate the electrochemistry of 2-OH-AC at a glassy carbon electrode in a range of positive potentials and to determine the optimum operating range of voltages for further EC/MS studies. In order to confirm the postulated oxidation mechanism of 2-OH-AC action and to identify the oxidation products, controlled-potential electrolysis of 2-OH-AC (0.5 mM in 0.02 M PBS buffer, pH 7.40) was performed at 0.50 V. To support the possibility of the formation of the stable adduct between 2-OH-AC intermediate and GSH, the tests were performed in the absence and the presence of GSH (5 mM in ultrapure water). The electrolysis measurements were carried out for 24 hours and the progress of the process was monitored periodically by application of voltammetric, spectroscopic, chromatographic, and spectrometric methods.

Data for the CV are provided in the supplemental material. In the solution of pure 2-OH-AC one anodic peak (a1) and three cathodic peaks (c1, c2, c3) were obtained. The appearance of three cathodic peaks indicated that the oxidation product of 2-OH-AC underwent subsequent chemical reactions. The addition of 10-fold excess of GSH to 2-OH-AC solution resulted in a shift of the oxidation peak of 2-OH-AC of about 30 mV to a more positive potential. In turn, the signal appearing in the cathodic part of the CV at circa 0.32 V virtually disappeared and two other cathodic peaks were substantially depressed. These

changes confirmed the interaction between 2-OH-AC and GSH, and the reducing effect of GSH against the oxidation reaction products.

Assuming that during oxidation process of 2-OH-AC two electrons are exchanged, the total electrolysis of 0.5 mM compound should be achieved at the time of obtaining the charge of 200 mC. Unfortunately, despite long electrolysis (over 1 day) the maximum charge which was achieved was only 29 mC. A possible explanation of this situation is that the oxidation products of 2-OH-AC strongly adsorbed on the electrode surface and effectively blocked it. With electrolysis progress the intensity of the current signals drastically decreased (Figure 2a). In addition, a new oxidation signal at circa 0.06 V (a2) was also well visible. It was related to the third cathodic peak (c1). The introduction of GSH to the solution of 2-OH-AC significantly minimized the effects of the electrolysis process. This observation may point out the presence of interactions between oxidation products of 2-OH-AC and GSH. The CPE of a mixture of 2-OH-AC and GSH (Figure 2b) revealed the anodic signal at circa 0.42 V (a1) with increasing intensity. Also a new signal emerged at circa 0.31 V (a2) and its height increased with time of electrolysis. This product peak was due to the reduction of the transformed 2-OH-AC molecule.

Electrochemical simulation of the oxidative metabolism of 2-OH-AC (phase I metabolism)

The electrochemical oxidation products of 2-OH-AC were generated and identified using on-line EC/MS (Figure 1a). The applied set up enabled us to simulate metabolic P450-catalyzed reactions occurring in the liver. To reduce the complexity of the system these experiments were carried out only with flow injection EC/MS without using an LC column.

The best electrochemical conversion of 2-OH-AC into its expected products was achieved using the scan mode in the potential range of 0 – 2.5 V. To provide a concise overview of the oxidation products, 2-D mass voltammograms were generated by plotting the extracted ion intensities versus the progress of the electrochemical oxidation. Mass spectrometry allowed the identification of the formed products by an increasing signal intensity of the corresponding mass-to-charge (*m/z*) ratio. Furthermore, for structure

elucidation of the detected products, fragment ions, generated by in-source fragmentation in the ESI interface, have been studied.

A representative 2-D mass voltammogram resulting from the oxidation of 2-OH-AC within the scanned range is shown in Figure 3. The 2-OH-AC molecule was easily protonated and detected with high intensities as $[M+H]^+$ ion (*m/z* 212) in the positive ionization mode of the ESI-Q-TOF mass spectrometer. No products were observed in the solution of pure 2-OH-AC without any electrochemical potential (cell off) (the inset of top left corner in Figure 3), whereas significant drop in an extracted ion intensity of 2-OH-AC was noticed when the potential was applied (cell on) (the inset of top right corner in Figure 3). This change is attributed to the oxidation of 2-OH-AC into eight products in an electrochemical thin-layer cell. All products are summarized in Table 2 and will be discussed in detail, with specific reference to their accurate mass data and fragmentation patterns.

Furthermore, we noticed that the ratios of oxidation products of 2-OH-AC were strongly dependent on the solvent composition. Most products identified using methanol-containing electrolyte, with the exception of P4 (*m/z* 240) and P8 (*m/z* 421), have been also observed in solutions of acetonitrile. No additional oxidation products of 2-OH-AC were detected under these conditions. Higher signal intensity of the selected mass ions was caused by that methanol was better than acetonitrile in diminishing the adsorption of the electrochemical products on the surface of the working electrode. Moreover, methanol/water electrolyte solution produced the lowest mass background noise in positive total ion chromatogram (data not shown). A summary of the electrochemical products observed under different electrolyte conditions is available in the supplemental material.

Characterization of GSH conjugate formed from electrochemical oxidation of 2-OH-AC (phase II metabolism)

In this work, the EC/MS set-up described above was extended to a system allowing the study of the conjugation of 2-OH-AC oxidation products with a reactive endogenous nucleophile, such as reduced GSH or NAC. GSH and NAC were selected because of a simple structure with their soft nucleophilic thiol group and their relevance in living organisms

(Evans *et al.* 2004). The instrumental set-up for electrochemical simulation of conjugation reactions (phase II reactions) is shown in Figure 1b.

Observation of the potential conjugation reaction(s) between the oxidation product(s) of 2-OH-AC and GSH was possible in the form of a 2-D mass voltammogram (Figure 4a).

The mass spectra were acquired to confirm the formation of GSH S-conjugate (Figure 5). As expected, no additional signals besides those associated with protonated 2-OH-AC (*m/z* 212) and GSH (*m/z* 308) were observed at cell off (Figure 5a and a zoom in the mass spectrum from the circle range). However, in the potential range of 0 – 2.5 V (cell on) mass spectrum revealed one *m/z* signal representing potential GSH S-conjugate (Figure 5b and a zoom in the mass spectrum from the circle range). Ion with a *m/z* ratio of 517 was observed with a weak intensity which was increasing only in the case when an extracted ion intensity of protonated 2-OH-AC was decreasing. It was confirmed by the accurate mass measurements that *m/z* 517 represents the conjugate of molecular formula $C_{23}H_{24}N_4O_8S$, consistent with a product of the 2-OH-AC oxidation and one molecule of GSH. This result is in accordance with the assumption that GSH traps soft electrophiles with its thiol group (Inoue *et al.* 2015).

To confirm that the ion at *m/z* 517 is originating from GSH conjugate of 2-OH-AC, the fragmentation spectrum was recorded (Figure 5c). The MS/MS of *m/z* 517 ion produced two fragment ions at *m/z* 388 and 244, respectively. The accurate values of *m/z* correlated well with calculated *m/z* (Table 3). The first was consistent with the neutral loss of anhydroglutamic acid (-129), whereas the second (-275) was assigned as a cleavage adjacent to the cysteinyl thioether moiety with charge retention on the 2-OH-AC molecule. Thus, the fragmentation pattern of *m/z* 517 ion suggested the presence of at least one GSH moiety. As for GSH, formation of NAC S-conjugate with a *m/z* ratio of 373 was also observed in similar experiments (Figure 4b). The MS/MS of 373 ion revealed the presence of the fragment ion at *m/z* 244 (data not shown), exactly the same that occurred in MS/MS of *m/z* 517 ion.

Identification of GSH conjugate of 2-OH-AC from in vitro microsomal incubations and controlled-potential electrolysis

Trapping experiments with GSH in *in vitro* microsomal incubations and during controlled-potential electrolysis of 2-OH-AC were carried out to generally assess the feasibility of GSH S-conjugate formation. The results obtained from these approaches were compared with those from a purely instrumental electrochemical simulation. Figure 6a presents the representative high performance LC chromatograms recorded for enzymatic and electrochemical oxidation of 2-OH-AC in the absence and the presence of 10-fold excess of GSH.

Due to various expressions of the different isoforms of P450 in each organism, the metabolism in human and rat liver microsomes may result in different metabolites or in a different quantitative distribution of the metabolites (Martignoni *et al.* 2006). When experiments were performed using both types of microsomal fractions, in the case of 2-OH-AC we observed only slight differences in the intensity of the individual peaks, hence the further discussion will be based on the results from RLM studies. The microsomal incubations included three controls, one without 2-OH-AC to rule out any potential interference/contamination from endogenous compounds, the second without NADPH, a cofactor for cytochrome P450 activities, to assess the metabolic dependence of GSH conjugate formation, and the third without GSH. No conjugate was detected in the “no compound’ and “no NADPH” control reactions (data shown in the supplemental material). LC analysis of microsomal samples without GSH revealed that three main metabolites were formed under the conditions studied (Figure 6a). Chromatogram taken after 60 min incubation of 2-OH-AC with 10-fold excess of GSH represents one additional chromatographic peak. It is noteworthy that it was not seen in the control incubations without NADPH, which suggests an NADPH-dependent oxidation of 2-OH-AC to this metabolite**.** LC analysis of the reaction mixture throughout the course of controlled-potential electrolysis revealed one main product (Figure 6a). Compared to enzymatically generated metabolites,

two of them were missing. As before, one additional peak was observed only where GSH was present in excess, and its intensity depended on the progress of electrolysis.

In both approaches the UV-Vis spectra of the peaks at 18.6 min differed significantly from that of the substrate (the inset in Figure 6a). The shift towards longer wavelengths may indicate that a more extensive delocalized electron system exists in this product in comparison to that in 2-OH-AC. It was subsequently identified by ESI-MS as GSH S-conjugate with the mass ion at *m/z* 517 (data not shown). Therefore, the above results agreed with the data obtained from EC/MS or EC/MS/MS measurements and confirmed the existence of a reactive intermediate in the oxidative pathway of 2-OH-AC. However, due to the low concentration of the S-conjugate in the EC/MS system it was not possible to obtain its chromatographic peak and UV-Vis spectrum. Also other products showing quite good intensities in the EC/MS system, were found in small or trace amounts in LC analysis (Figure 6b). Some of them were not detected, which is likely to be a consequence of their low stability. Nevertheless, it is worth to note that generally the EC system allowed to obtain a wider set of phase I metabolites than the use of classical approaches, probably because of clean matrix.

Discussion

The toxic effects of drugs and other xenobiotics arise not only from the compound itself but also from its metabolites (Baumann *et al.* 2010). Hence, during drug development process particular attention is paid to drug metabolite formation and identification of metabolic pathways. Progress in this research area depends critically on the improvement of methods involved in the generation and analysis of various types of drug metabolites, with special respect to the characterization of reactive metabolites (Prakash *et al.* 2008). In this work different approaches for the investigation of the 2-OH-AC oxidative metabolism, that may occurs in the living organism, were performed. The oxidative electrochemical behavior of 2-OH-AC was first investigated by the direct combination of electrochemistry and mass spectrometry. The applicability of the electrochemistry in drug metabolite synthesis was evaluated by conventional electrochemical (controlled-potential electrolysis) and enzymatic (microsomal incubation) approaches.

The electrochemical conversion of 2-OH-AC in an electrochemical thin-layer cell was successfully achieved (Figure 3). Table 2 consists of list of major products related to 2-OH-AC oxidative metabolism and *m/z* ratios of the protonated species $[M+H]^+$ used for mass spectra interpretation. The resulting molecular formulas were deduced by their accurate masses. The isotopic patterns correlated well with theoretical calculations. For all compounds, the deviations between the calculated and measured *m/z* values were less than 4 ppm.

The proposed chemical reactions that may occur in the electrochemical cell are summarized in Figure 7. Most of 2-OH-AC oxidation products seem to be species containing additional oxygen atom and can exist in at least two tautomeric forms. According to previous studies on the oxidative transformations of 2-OH-AC (Mazerska *et al.* 2002), the most likely oxidation site in the 2-OH-AC molecule is the position *ortho* to the hydroxyl group. This relates to the positions 1 or 3 of 2-OH-AC, wherein position 1 remains preferential. Thus, the mass ion at *m/z* 226 is proposed to correspond to 1,2-orthoquinone (P1a), while the signal at *m/z* 228 may include monohydroxylation product (P3). The molecular ion observed with little

signal intensity at *m/z* 421 was identified to be the dimer formed from two substrate molecules of radical structure linked together at position 1 of 2-OH-AC (P8). The chemical structures of these three products have been previously determined by means of MS and NMR spectroscopy (Mazerska *et al.* 2002).

Other products of oxidative metabolism of 2-OH-AC have been identified for the first time upon electrochemical oxidation. The P2 compound with the mass ion at *m/z* 227 may have been formed via *C*- or *N*-hydroxylation because the mass corresponds to an addition of 15.99 Da to the parent compound with a lack of one hydrogen atom. As a result, the P2 molecule should contain a positive charge, probably located on the nitrogen atom of the acridinone ring. Further, considering the mesomeric effects in electron density distribution, the loss of one hydrogen atom in P2 compound would indicate the possibility of the formation other than P1a structures for the mass ion at *m/z* 226, including P1b.

The products showing the mass ions at *m/z* 240 (P4), 242 (P5), 256 (P6), and 258 (P7) have not been definitively identified. However, we propose here only their tentative structures. The accurate mass of ion at *m/z* 242 (P5) differed from the accurate mass of ion at *m/z* 226 (P1) by exactly 16.03 Da. This value may indicate the presence of the additional one carbon and four hydrogen atoms, but not a single oxygen atom (15.99 Da), somewhere within the P5 molecule. During the electrochemical and/or the ionization processes some side reactions can take place, like the reaction of electrolyte components with electrochemically generated intermediates and sometimes they are unexpected. Based on the literature data (Sichilongo *et al.* 2011; Wang *et al.* 2011), electro-oxidation of methanol from electrolyte may give a strongly electrophilic methylium (CH_3^+) or methyl radical ($\bullet CH_3$). Thus, we can assume that it is quite likely that compound containing a methyl group in its structure was formed. The probable methylation of 2-OH-AC derivative have not been avoided even when acetonitrile was present in the electrolyte solution (supplemental material). The possible location of attachment is speculated to be an electronegative nitrogen atom due to valence considerations. Presumably further two-electron two-proton dehydrogenation of P5 provided P4 (*m/z* 240), with molecular mass ion decreased by 2.01

Da. In turn, a product with the mass ion at *m/z* 258 (P7) could have been created by the hydroxylation of the methyl group of P5, and its further two-electron two-proton dehydrogenation gave a signal at *m/z* 256 (P6).

It should be pointed out that the signals at *m/z* 240 and *m/z* 256 may correspond to aldehyde products as well. To test whether the hydroxymethyl group at the nitrogen atom in P5 or in P7 products underwent further oxidation, trapping experiments were performed with semicarbazide. It is a small molecule trapping agent that can form a Schiff base with aldehydes in the process mimicking reactions between aldehyde metabolites with lysine residues on proteins (Evans *et al.* 2004). Semicarbazide was added to the electrochemical oxidation mixture of 2-OH-AC followed by LC/MS analysis. Trapping with semicarbazide did not give any conjugates what excluded the presence of aldehyde products in oxidative transformations of 2-OH-AC.

To simulate the phase II metabolism of 2-OH-AC, electrochemical oxidation of the compound was carried out in the presence of an excess amount of nucleophilic trapping agent. EC/MS successfully predicted the formation of chemically reactive metabolite that spontaneously reacted with reduced glutathione (Figures 4a and 5) and/or *N*-acetylcysteine (Figure 4b) to form conjugates (*m/z* 517 and *m/z* 373, respectively) via the thiol group. General structures for probable GSH and NAC conjugates of 2-OH-AC are shown in Figure 8. We suspect that 2-OH-AC is likely to undergo a P450-catalyzed oxidative dehydrogenation which results in the formation of a reactive intermediate in the form of a quinone imine (Guengerich 2007), as, *e.g.*, it takes place in a metabolic pathway of the acetaminophen (Jollow *et al.* 1973; Larson 2007). For this mechanism, a quinone imine of 2-OH-AC has to be the precursor of the adduct as the corresponding quinone imine would have the *m/z* ratio of 210 in the positive-ion mode detection. However, this intermediate product, presumably due to its short life span and high reactivity, was not directly detected in the mass voltammogram of pure 2-OH-AC. It is important to note that the same type of GSH S-conjugate was detected after *in vitro* liver microsomal incubations in an NADPH-dependent manner and in the reaction mixture from the electrolysis experiment (Figure 6). Quinone

imines are well known reactive intermediates which very often undergo adduct formation with crucial cellular compounds such as GSH, structural proteins, enzymes and/or DNA (Bolton *et al.* 2000; Zhou *et al.* 2005). As a consequence, these compounds can cause a variety of hazardous effects *in vivo*, including acute cytotoxicity, immunotoxicity, and carcinogenesis, especially in the case of depleted levels of cellular GSH (Lohmann *et al.* 2010). However, the fact that reactive metabolite of 2-OH-AC may exist and, as it has been shown, may undergo adduct formation does not consequently imply that it causes toxicity (Evans *et al.* 2004) so further studies are needed to elucidate whether this metabolite contributes to the 2-OH-AC toxicity *in vivo*.

The results of our studies clearly prove that EC-based approach has the potential to simulate the majority of oxidative metabolism reaction, including the simulation of reactive metabolite formation and its binding to biomolecules (*e.g.*, GSH). The observed dehydrogenation, hydroxylation and oxidation of acridinone molecule are in general agreement with reports on the types of P450-catalyzed reactions being simulated by electrochemistry (Lohmann & Karst 2008; Lohmann *et al.* 2010). Our observations on product structures may be advantageous from the viewpoint of the structural factors that influence the reactivity and functional group interactions of the compound, providing a good approximation of what may occur *in vivo*.

Conclusions

The present study demonstrated the significance of electrochemistry coupled on-line with mass spectrometry in drug metabolism studies. This combination appeared to be a suitable tool for a simulation of some types of oxidative drug metabolic reactions related to cytochromes P450, and for studying the formation of reactive metabolites. In this investigation, 2-hydroxyacridinone (2-OH-AC), the reference compound for antitumor-active imidazo- and triazoloacridinone derivatives, was easily oxidized in an electrochemical thin-layer cell to several different products. To trap potentially reactive metabolite(s) two types of nucleophilic trapping agents, reduced GSH and NAC, both with nucleophilic thiol group, were used. This allowed us to identify and characterize a novel GSH (NAC) S-conjugate of 2-OH-AC. The postulated reactive quinone imine metabolite of 2-OH-AC may potentially be involved in a number of biochemical transformations, and can be responsible for the antitumor activity of acridinone derivatives. The role of this reactive metabolite requires further investigation.

The electrochemical method we proposed here represented a good alternative for classical metabolic studies with the principal advantage which is the absence of proteins in the reaction medium. It will be very useful in further studies on metabolic transformations of antitumor imidazo- and triazoloacridinone drugs. Considering pharmacological aspect, our findings may provide important guidelines for the further modification of the acridinone compounds so they contribute to the design and the development of safer and more effective therapeutic agents.

Acknowledgments

This work was supported by the National Science Center (Poland) under Grant number 2012/07/D/NZ7/03395..

Declaration of interest statement

The authors confirm that this article content has no conflicts of interest.

References

Acheson RM. (1973). Acridines. In: Acheson RM, ed. The chemistry of heterocyclic compounds. New York, Interscience Publishers, Inc., p. 141.

Augustin E, Mość-Rompa A, Skwarska A, Witkowski JM, Konopa J. (2006). Induction of G2/M phase arrest and apoptosis of human leukemia cells by potent antitumor triazoloacridinone C-1305. Biochem Pharmacol 72: 1668-1679.

Baillie TA, Cayen MN, Fouda H, Gerson RJ, Green JD, Grossman SJ, *et al.* (2002). Drug metabolites in safety testing. Toxicol Appl Pharmacol 182: 188-196.

Baumann A, Lohmann W, Rose T, Ahn KC, Hammock BD, Karst U, *et al*. (2010). Electrochemistry-mass spectrometry unveils the formation of reactive triclocarban metabolites. Drug Metab Dispos 38: 2130-2138.

Bolton JL, Trush MA, Penning TM, Dryhurst G, Monks TJ. (2000). Role of quinones in toxicology. Chem Res Toxicol 13: 135-160.

Brandon EF, Raap CD, Meijerman I, Beijnen JH, Schellens JH. (2003). An update on in vitro test methods in human hepatic drug biotransformation research: pros and cons. Toxicol Appl Pharmacol 189: 233-246.

Bussy U, Boisseau R, Thobie-Gautier C, Boujtita M. (2015). Electrochemistry-mass spectrometry to study reactive drug metabolites and CYP450 simulations. Trends Anal Chem 70: 67-73.

Bussy U, Boujtita M. (2014). Advances in the electrochemical simulation of oxidation reactions mediated by cytochrome P450. Chem Res Toxicol 27: 1652-1668.

Cholody WM, Horowska B, Paradziej-Lukowicz J, Martelli S, Konopa J. 1996. Structure-activity relationship for antineoplastic imidazoacridinones: synthesis and antileukemic activity in vivo. J Med Chem 39: 1028-1032.

Cholody WM, Martelli S, Konopa J. (1990). 8-Substitued 5-[(aminoalkyl)amino]-6H-v-triazolo[4,5,1-de]acridin-6-ones as potential antineoplastic agents. Synthesis and biological activity. J Med Chem 33: 2852-2856.

Cholody WM, Martelli S, Lukowicz J, Konopa J. (1990). 5-[(Aminoalkyl)amino]imidazo[4,5,1-de]acridin-6-ones as a novel class of antineoplastic agents. Synthesis and biological activity. J Med Chem 33: 49-52.

Dziegielewski J, Konopa J. (1996). Interstrand crosslinking of DNA induced in tumor cells by a new group of antitumor imidazoacridinones. Proc Am Assoc Cancer Res 37: 410.

Dziegielewski J, Konopa J. (1998). Characterisation of covalent binding to DNA of antitumor imidazoacridinone C-1311, after metabolic activation. Ann Oncol Suppl 1: 137.

Dziegielewski J, Slusarski B, Konitz A, Skladanowski A, Konopa J. (2002). Intercalation of imidazoacridinones to DNA and its relevance to cytotoxic and antitumor activity. Biochem Pharmacol 63: 1653-1662.

Evans DC, Watt AP, Nicoll-Griffith DA, Baillie TA. (2004). Drug-protein adducts: An industry perspective on minimizing the potential for drug bioactivation in drug discovery and development. Chem Res Toxicol 17: 3-16.

Faber H, Jahn S, Kunnemeyer J, Simon H, Melles D, Vogel M, *et al.* (2011). Electrochemistry/liquid chromatography/mass spectrometry as a tool in metabolism studies. Angew Chem 50: A52-58.

Guengerich FP. (2007). Oxidative, reductive and hydrolytic metabolism of drugs. In: Zhang D, Zhu M, Humphreys WG, eds. Drug metabolism in drug design and development. New York, John Willey & Sons, Inc., p. 265.

Harding MM, Grummitt AR. (2003). 9-hydroxyellipticine and derivatives as chemotherapy agents. Mini Rev Med Chem 3: 67-76.

Inoue K, Fukuda K, Yoshimura T, Kusano K. (2015). Comparison of the reactivity of trapping reagents toward electrophiles: cysteine derivatives can be bifunctional trapping reagents. Chem Res Toxicol 28: 1546-1555.

Jennings GS, Strauss M. (1999). Immortalization of hepatocytes through targeted deregulation of the cell cycle. In: Al-Rubeai M, ed. Cell engineering. the Netherlands, Kluwer Academic Publishers, p. 259.

Jollow DJ, Mitchell JR, Potter WZ, Davis DC, Gillette JR, Brodie BB. (1973). Acetaminophen-induced hepatic necrosis. II. Role of covalent binding in vivo. J Pharmacol Exp Ther 187: 195-202.

Jurva U, Wikstrom HV, Weidolf L, Bruins AP. (2003). Comparison between electrochemistry/mass spectrometry and cytochrome P450 catalyzed oxidation reactions. Rapid Commun Mass Spectrom 17: 800-810.

Kalgutkar AS, Soglia JR. (2005). Minimising the potential for metabolic activation in drug discovery. Expert Opin Drug Metab Toxicol 1: 91-142.

Koba M, Konopa J. (2007). Interactions of antitumor triazoloacridinones with DNA,. Acta Biochim Pol 54: 297-306.

Kusnierczyk H, Cholody WM, Paradziej-Lukowicz J, Radzikowski C, Konopa J. (1994). Experimental antitumor activity and toxicity of the selected triazolo- and imidazoacridinones. Arch Immunol Ther Exper (Warsz) 42: 415-423.

Larson AM. (2007). Acetaminophen hepatotoxicity. Clin Liver Dis 11: 525-548.

Lemke K, Wojciechowski M, Laine W, Bailly C, Colson P, Baginski M, *et al.* (2005). Induction of unique structural changes in guanine-rich DNA regions by the triazoloacridone C-1305, a topoisomerase II inhibitor with antitumor activities. Nucleic Acids Res 33: 6034-6047.

Lohmann W, Karst U. (2008). Biomimetic modeling of oxidative drug metabolism: strategies, advantages and limitations. Anal Bioanal Chem 391: 79-96.

Lohmann W, Baumann A, Karst U. (2010). Electrochemistry and LC-MS for metabolite generation and identification: tools, technologies and trends. LC•GC Europe January: 1-7.

Marks TA, Venditti JM. (1976). Potentiation of actinomycin D or adriamycin antitumor activity with DNA. Cancer Research 36: 496-504.

Martignoni M, Groothuis GM, de Kanter R. (2006). Species differences between mouse, rat, dog, monkey and human CYP-mediated drug metabolism, inhibition and induction. Expert Opin Drug Metab Toxicol 2: 875-894.

Mazerska Z, Dziegielewski J, Konopa J. (2001). Enzymatic activation of a new antitumour drug 5-diethylaminoethylamino-8-hydroxyimidazo-acridinine, C-1311, observed after its intercalation into DNA. Biochem Pharmacol 61: 685-694.

Mazerska Z, Zamponi S, Marassi R, Martelli S, Konopa J. (1997). Electrochemical oxidation of antitumor imidazoacridinone derivatives and the reference 2-hydroxyacridinone. J. Electroanal Chem 427: 71-78.

Mazerska Z, Zamponi S, Marassi R, Sowinski P, Konopa J. (2002). The products of electro- and photochemical oxidation of 2-hydroxyacridinone, the reference compound of antitumor imidazoacridinone derivatives. J Electroanal Chem 521: 144-154.

Nouri-Nigjeh E, Bischoff R, Bruins AP, Permentier HP. (2011). Electrochemistry in the mimicry of oxidative drug metabolism by cytochrome P450s. Curr Drug Metab 12: 359-371.

Orhan H, Vermeulen NPE. (2011). Conventional and novel approaches in generating and characterization of reactive intermediates from drugs/drug candidates. Curr Drug Metab 12: 383-394.

Park BK, Boobis A, Clarke S, Goldring CE, Jones D, Kenna JG, *et al.* (2011). Managing the challenge of chemically reactive metabolites in drug development. Nat Rev Drug Discov 10: 292-306.

Permentier HP, Bruins AP, Bischoff R. (2008). Electrochemistry-mass spectrometry in drug metabolism and protein research. Mini Rev Med Chem 8: 45-56.

Pinto N, Dolan ME. (2011). Clinically relevant genetic variations in drug metabolizing enzymes. Curr Drug Metab 12: 487-497.

Prakash C, Sharma R, Gleave M, Nedderman A. (2008). In vitro screening techniques for reactive metabolites for minimizing bioactivation potential in drug discovery. Curr Drug Metab 9: 952-964.

Sichilongo KF, Famuyiwa SO, R. Kibechu R. (2011). Pre-electrospray ionisation manifold methylation and post-electrospray ionisation manifold cleavage/ion cluster formation observed during electrospray ionisation of chloramphenicol in solutions of methanol and acetonitrile for liquid chromatography-mass spectrometry employing a commercial quadrupole ion trap mass analyser. Eur J Mass Spectrom (Chichester) 17: 255-264.

Skladanowski A, Plisov SY, Konopa J, Larsen AK. (1996). Inhibition of DNA topoisomerase II by imidazoacridinones, new antineoplastic agents with strong activity against solid tumors. Mol Pharmacol 49: 772-780.

Srivastava A, Maggs JL, Antoine DJ, Williams DP, Smith DA, Park BK. (2010). Role of reactive metabolites in drug-induced hepatotoxicity. Handb Exp Pharmacol 196 (2010) 165-194.

Volk KJ, Yost RA, Brajter-Toth A. (1992). Electrochemistry on line with mass spectrometry insight into biological redox reactions. Anal Chem 64: 21A-26A.

Wang L, Chai Y, Tu P, Sun C, Pan Y. (2011). Formation of [M + 15](+) ions from aromatic aldehydes by use of methanol: in-source aldolization reaction in electrospray ionization mass spectrometry. J Mass Spectrom 46: 1203-1210.

Zanger UM, Schwab M. (2013). Cytochrome P450 enzymes in drug metabolism: Regulation of gene expression, enzyme activities, and impact of genetic variation. Pharmacol Therapeut 138: 103-141.

Zhou S, Chan E, Duan W, Huang M, Chen YZ. (2005). Drug bioactivation, covalent binding to target proteins and toxicity relevance. Drug Metab Rev 37: 41-213.

Tables with captions

Table 1

EC and ESI-Q-TOF-MS(/MS) parameters as applied in direct EC/MS(/MS) and in MS(/MS) experiments for determination of accurate masses of product ions and getting ion fragmentation.

	Parameter	Value or setting
EC settings	Flow rate	30 µL·min^{-1}
	Potential	0 – 2.5 V (10 mV steps)
	EC operating mode	scan
	Cycle	continuous
MS(/MS) settings	The range of *m/z*	100 – 600
	Ion source	dual ESI
	Ion polarity	positive
	MS operating mode	scan
	Capillary voltage	3500 V
	Nebulizer gas (N_2) pressure	35 psig
	Drying gas (N_2) flow	10 L·min^{-1}
	Drying gas temperature	325 °C
	Fragmentor	175 V
	Skimmer	45 V
	OCT 1 RF Vpp	750 V
	Rate	1,5 spectra·s^{-1}
	MS/MS method - Slope - Offset	targeted - 4 *m/z* - 5 V

Table 2

A summary of molecular formulas of 2-OH-AC and its products found after electrochemical oxidation on a GC working electrode in a potential range of 0 – 2.5 V versus Pd/H_2. Base fragment ions are shown in bold.

Product	Measured *m/z* / Da	Calculated *m/z* / Da [a]	Deviation / ppm	Molecular formula of $[M+H]^+$ ion	MS/MS fragment ions	Predicted modification of 2-OH-AC molecule
2-OH-AC	212.0712	212.0706	2.9	$C_{13}H_{10}NO_2$	-	-
P1a, b	226.0501	226.0499	1.1	$C_{13}H_8NO_3$	212	- 2H + O
P2	227.0578	227.0577	0.5	$C_{13}H_9NO_3$	212	- H + O
P3	228.0648	228.0655	-3.1	$C_{13}H_{10}NO_3$	212, 226, **227**	+ O
P4	240.0658	240.0655	1.2	$C_{14}H_{10}NO_3$	212, **227**, 228	+ CO
P5	242.0818	242.0812	2.6	$C_{14}H_{12}NO_3$	212, **228**, 240	+ 2H + CO
P6	256.0614	256.0604	3.8	$C_{14}H_{10}NO_4$	212, 226, **228**, 240, 242	+ CO_2
P7	258.0758	258.0761	-1.2	$C_{14}H_{12}NO_4$	212, 226, **228**, 240, 242, 256	+ 2H + CO_2
P8	421.1176	421.1183	-1.6	$C_{26}H_{17}N_2O_4$	212	2-OH-AC dimer

[a] Calculated using Molecular Mass Calculator freeware version v2.02.

Table 3

A summary of neutral losses and fragmentations for ions attributed to the respective glutathione S-conjugate of the 2-OH-AC.

MS/MS collision-induced dissociation of glutathione S-conjugate			2-OH-AC		
			Measured *m/z* / Da	Calculated *m/z* / Da [a]	Deviation / ppm
Neutral losses	Parent	*m/z* / Da	517.1382	517.1387	1.04
	Glycine	75.0320	None	442.1067	None
	Anhydroglutamic acid	129.0426	388.0963	388.0962	-0.39
	Glutamine	146.0691	None	371.0696	None
	γ-Glu-Ala-Gly	275.1117	244.0421 [b]	244.0427	2.34
	Glutathione (S-oxide)	322.0709	None	195.0679	None

[a] Calculated using Molecular Mass Calculator freeware version v2.02.
[b] Neutral loss of γ-Glu-Ala-Gly + 2H.

Figure captions

Figure 1

Instrumental set-ups used for (**a**) the electrochemical simulation of the oxidative metabolism of 2-OH-AC and (**b**) the investigation of the reactivity of 2-OH-AC oxidation products towards GSH (NAC).

Legend: 1 – infusion syringe pump, 2 – potentiostat, 3 – electrochemical thin-layer cell (EC) – reactor cell, 4 – mass spectrometer (MS), 5 – T-piece and 100 µL mixing coil

Chemical structures of the investigated 2-hydroxyacridinone (2-OH-AC) compound and glutathione (GSH)/*N*-acetylcysteine (NAC)**,** used as nucleophilic trapping agents, are presented in the frame.

Figure 2

Cyclic voltammograms of 0.5 mM 2-OH-AC (**a**) alone and (**b**) in the mixture with 5 mM GSH in 0.02 M PBS buffer, pH 7.40, versus electrolysis progress. Experimental conditions: potential range -0.2 – 1.2 V; scan rate 100 $mV \cdot s^{-1}$; T = 21 ^{o}C; ϕ GC 3 mm.

Figure 3

Two-dimensional plot (2-D mass voltammogram) of 10 µM 2-OH-AC oxidation at a GC working electrode (extracted ion intensity versus the progress of the electrochemical oxidation; positive-ion mode). The *m/z* ratios shown correspond to the protonated 2-OH-AC and its products (see legend). Experimental conditions: potential range 0 – 2.5 V; scan rate 10 $mV \cdot s^{-1}$, continuous; T = 21 ^{o}C; ϕ GC 8 mm. The insets show the representative mass spectrum of 2-OH-AC without voltage applied to the electrochemical cell (cell off; top left corner) and after electrochemical oxidation (cell on; top right corner).

Figure 4

Two-dimensional plots (2-D mass voltammograms) of 10 µM 2-OH-AC oxidation at a GC working electrode in the presence of 100 µM (a) GSH and (b) NAC (extracted ion intensity versus the progress of the electrochemical oxidation; positive-ion mode). The *m/z* ratios shown correspond to the protonated 2-OH-AC and GSH or NAC S-conjugate (see legend).

Experimental conditions: potential range 0 – 2.5 V; scan rate 10 $mV \cdot s^{-1}$, continuous; T = 21 ^{o}C; ϕ GC 8 mm.

Figure 5

The representative mass spectrum of a mixture of 2-OH-AC and GSH (**a**) without voltage applied to the electrochemical cell (cell off) and (**b**) after electrochemical oxidation (cell on). The insets show a zoom in the mass range from *m/z* 510 to 520 (positive-ion mode). (**c**) Fragmentation spectrum of the conjugation product *m/z* 517.

Figure 6

(**a**) The representative high performance LC chromatograms of the reaction mixtures obtained after metabolism simulation of 0.5 mM 2-OH-AC in the absence (black line) and the presence (grey dashed line) of 5 mM GSH in RLM incubations (enzymatic oxidation) and from controlled-potential electrolysis (oxidation by CPE). The inset shows UV-Vis spectra of GSH S-conjugate and 2-OH-AC. (**b**) The representative extracted ion chromatograms for 2-OH-AC oxidation in electrochemical cell.

Figure 7

Proposed oxidation reaction pathways of 2-OH-AC observed in the electrochemical cell. Tentative structures were derived on the basis of accurate mass measurements and MS/MS fragmentation patterns. Probable isomeric compounds are gathered in encircled blocks.

Figure 8

Schematic representation of the proposed mechanism of the 2-OH-AC electrochemical oxidation and GSH (NAC) S-conjugate formation.

Figure 1

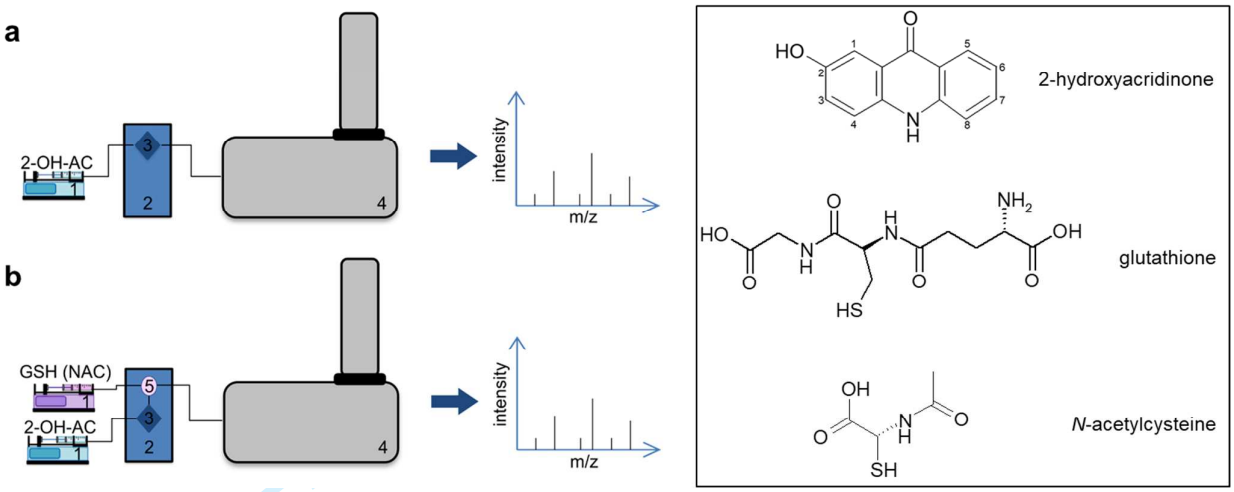

Figure 2

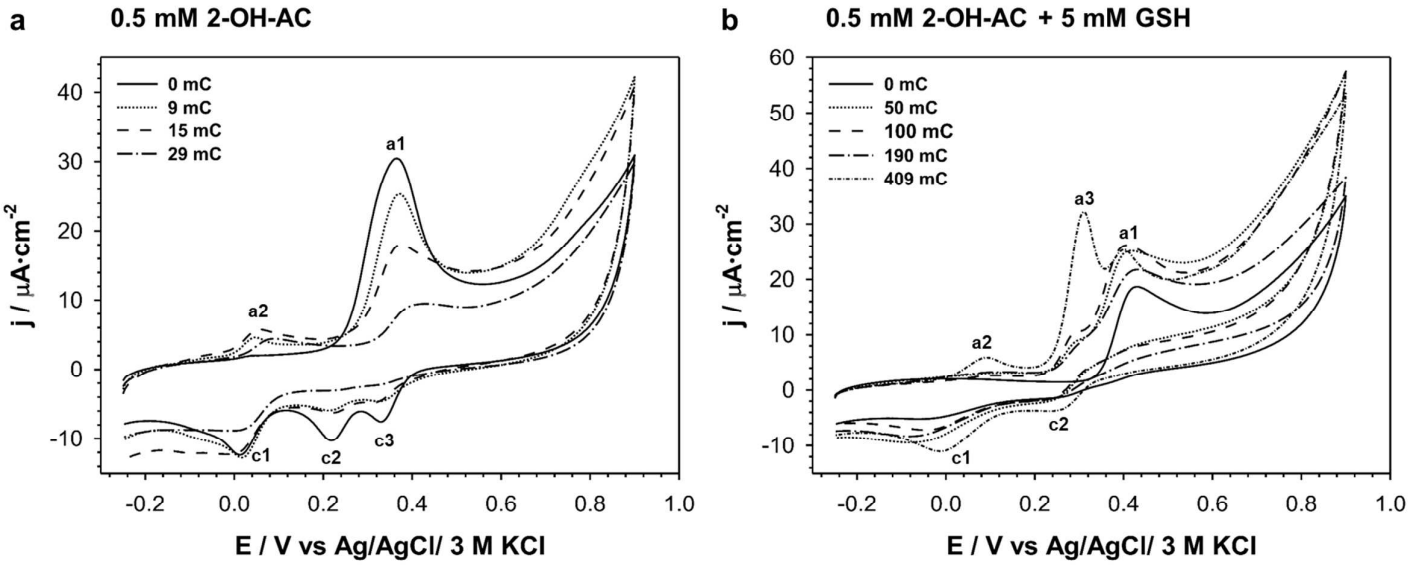

Figure 3

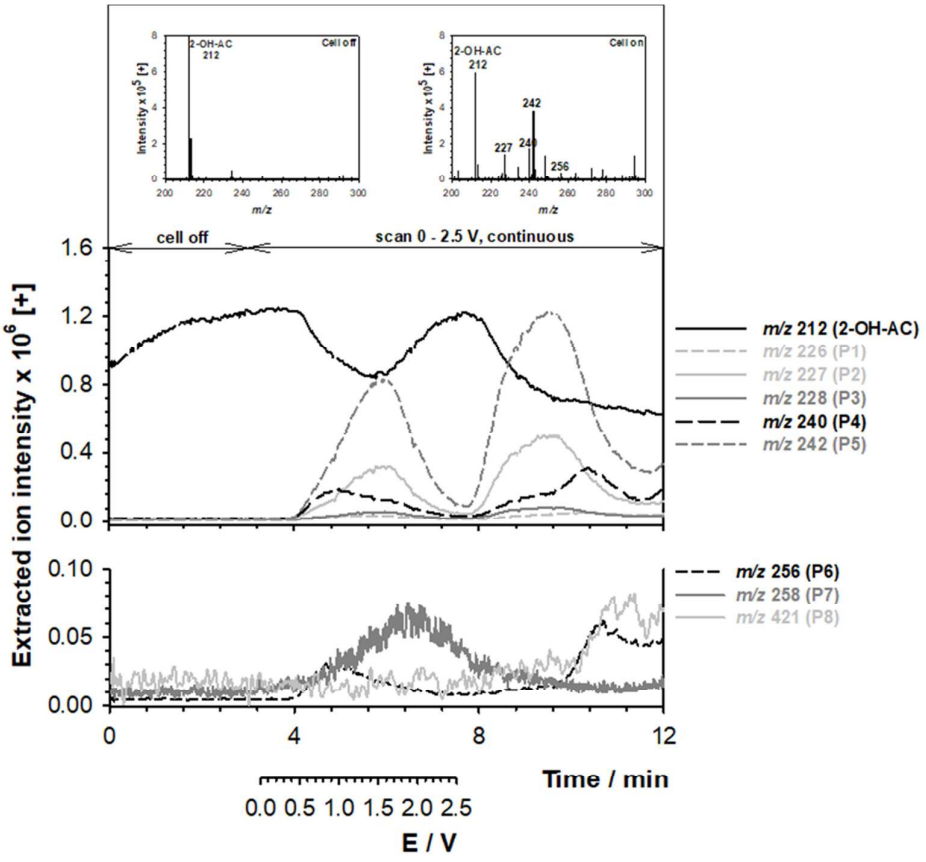

Figure 4

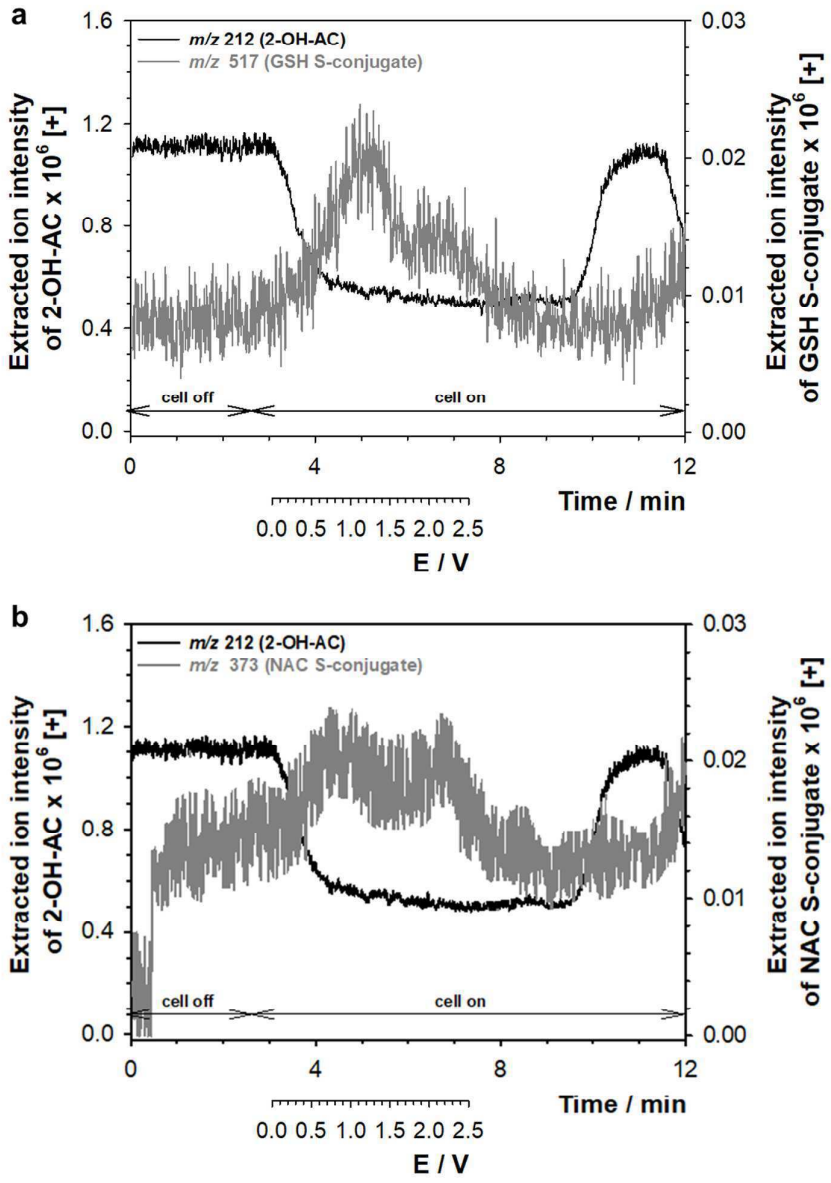
a
m/z 212 (2-OH-AC)
m/z 517 (GSH S-conjugate)
Extracted ion intensity of 2-OH-AC x 10^6 [+]
Extracted ion intensity of GSH S-conjugate x 10^6 [+]
cell off
cell on
Time / min
E / V
b
m/z 212 (2-OH-AC)
m/z 373 (NAC S-conjugate)
Extracted ion intensity of 2-OH-AC x 10^6 [+]
Extracted ion intensity of NAC S-conjugate x 10^6 [+]
cell off
cell on
Time / min
E / V

Figure 5

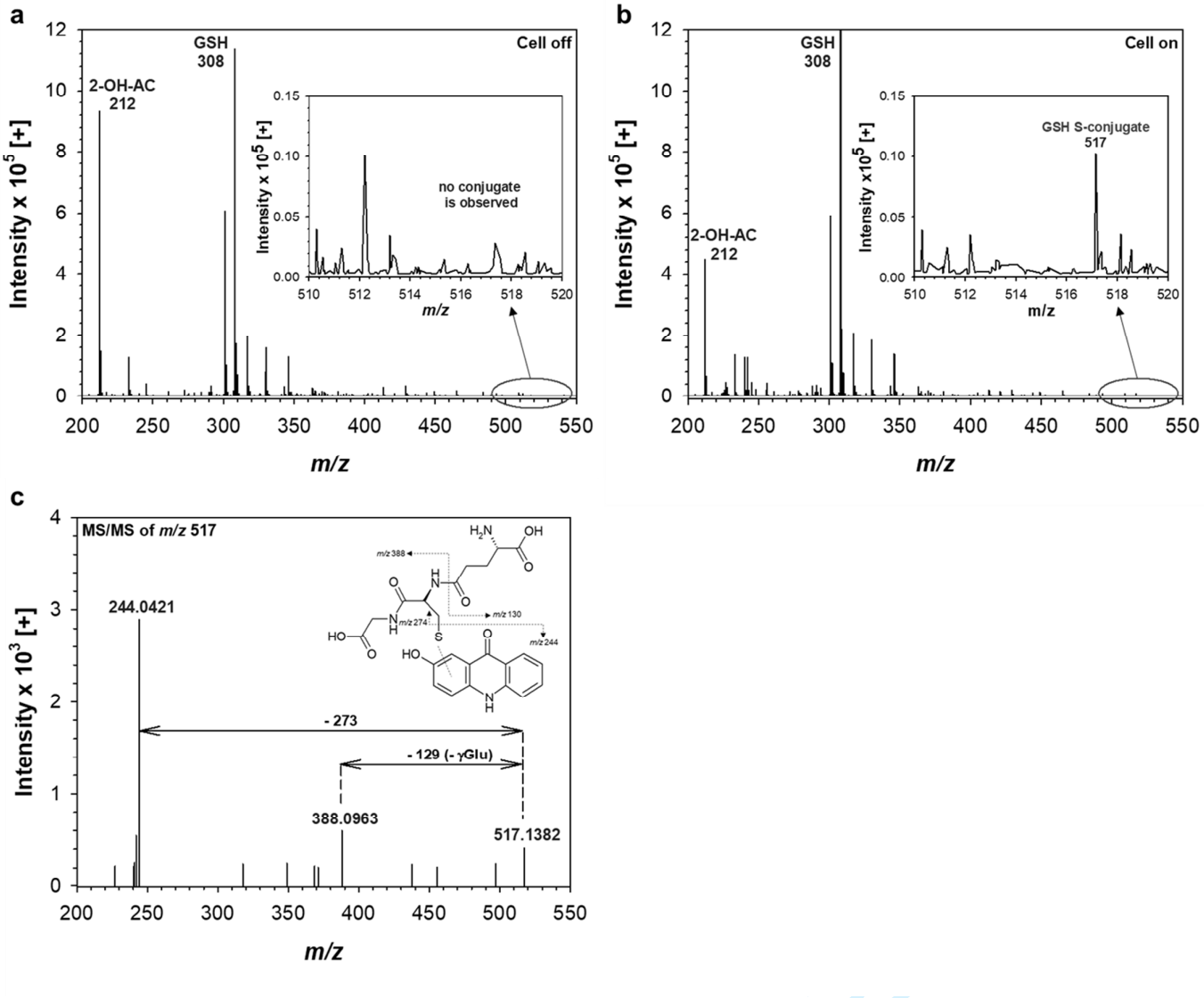
a
Cell off
GSH
308
2-OH-AC
212
no conjugate
is observed
Intensity x 10^5 [+]
m/z
b
Cell on
GSH
308
2-OH-AC
212
GSH S-conjugate
517
Intensity x 10^5 [+]
m/z
c
MS/MS of m/z 517
244.0421
- 273
- 129 (- γGlu)
388.0963
517.1382
Intensity x 10^3 [+]
m/z

Figure 6

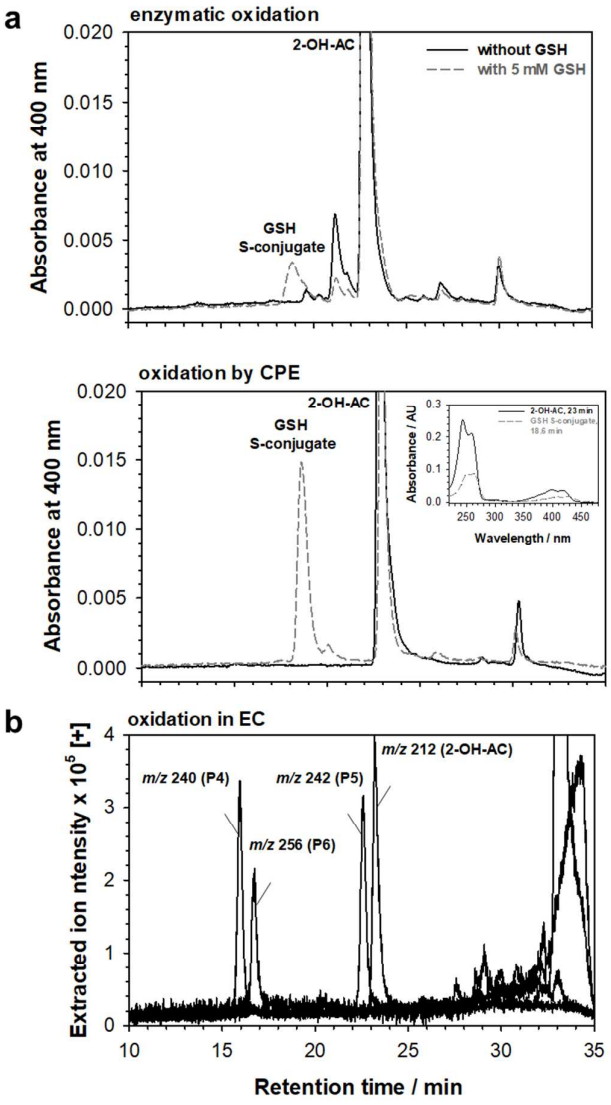

Figure 7

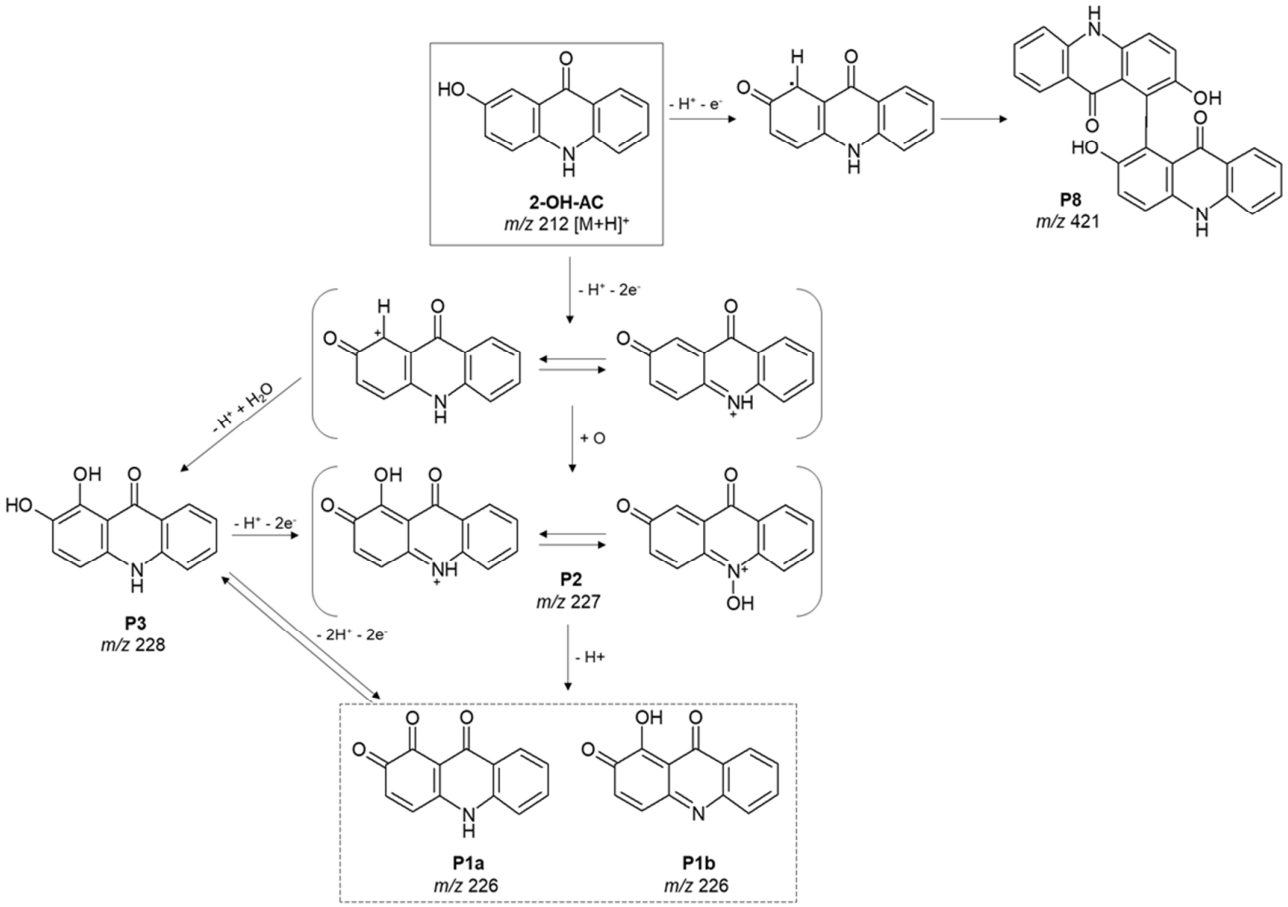

Figure 8

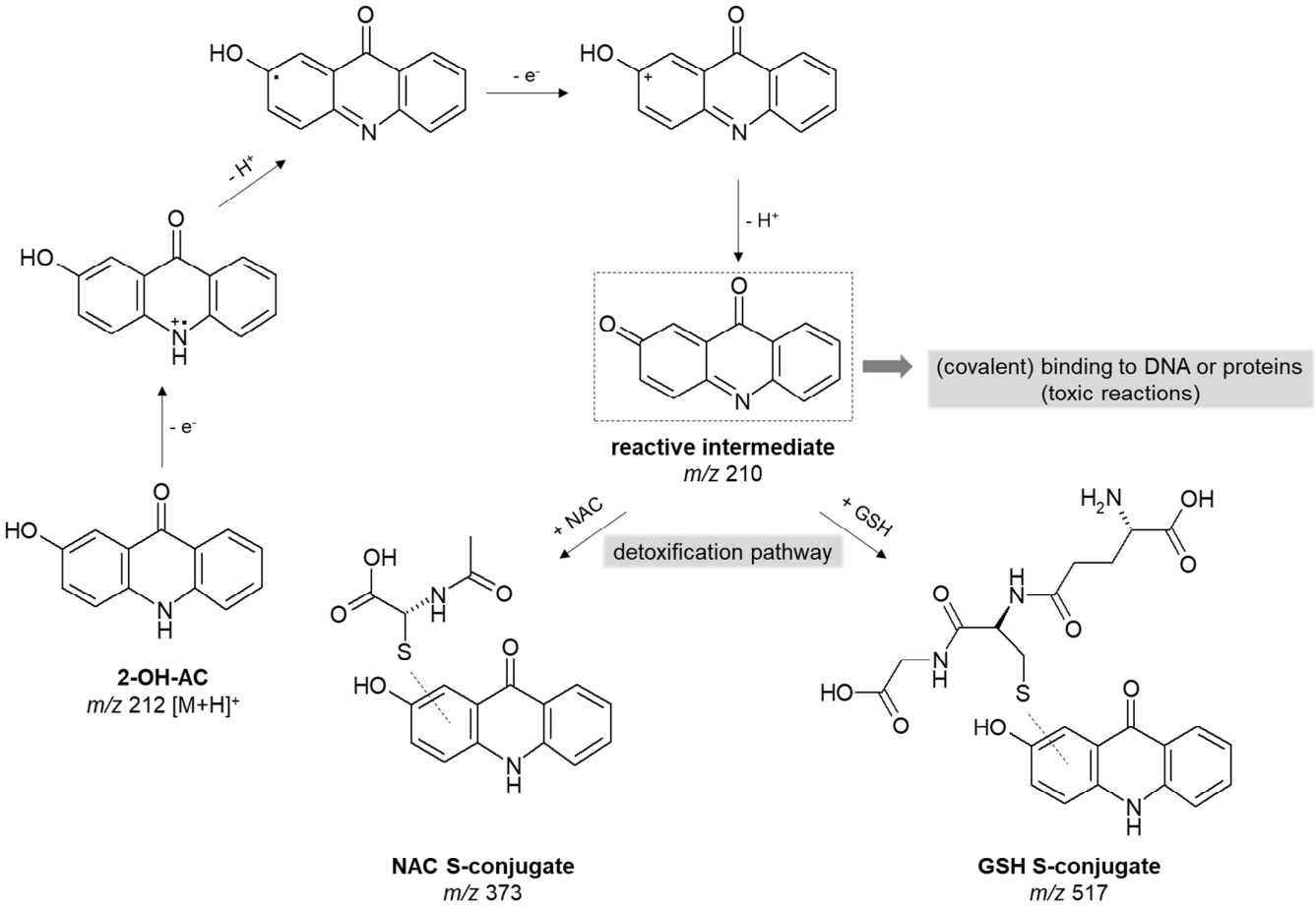

Table 1

	Parameter	Value or setting
EC settings	Flow rate	30 µL·min^{-1}
	Potential	0 – 2.5 V (10 mV steps)
	EC operating mode	scan
	Cycle	continuous
MS(/MS) settings	The range of *m/z*	100 – 600
	Ion source	dual ESI
	Ion polarity	positive
	MS operating mode	scan
	Capillary voltage	3500 V
	Nebulizer gas (N_2) pressure	35 psig
	Drying gas (N_2) flow	10 L·min^{-1}
	Drying gas temperature	325 °C
	Fragmentor	175 V
	Skimmer	45 V
	OCT 1 RF Vpp	750 V
	Rate	1,5 spectra·s^{-1}
	MS/MS method - Slope - Offset	targeted - 4 *m/z* - 5 V

Table 2

Product	Measured *m/z* / Da	Calculated *m/z* / Da [a]	Deviation / ppm	Molecular formula of $[M+H]^+$ ion	MS/MS fragment ions	Predicted modification of 2-OH-AC molecule
2-OH-AC	212.0712	212.0706	2.9	$C_{13}H_{10}NO_2$	-	-
P1a, b	226.0501	226.0499	1.1	$C_{13}H_8NO_3$	212	- 2H + O
P2	227.0578	227.0577	0.5	$C_{13}H_9NO_3$	212	- H + O
P3	228.0648	228.0655	-3.1	$C_{13}H_{10}NO_3$	212, 226, **227**	+ O
P4	240.0658	240.0655	1.2	$C_{14}H_{10}NO_3$	212, **227**, 228	+ CO
P5	242.0818	242.0812	2.6	$C_{14}H_{12}NO_3$	212, **228**, 240	+ 2H + CO
P6	256.0614	256.0604	3.8	$C_{14}H_{10}NO_4$	212, 226, **228**, 240, 242	+ CO_2
P7	258.0758	258.0761	-1.2	$C_{14}H_{12}NO_4$	212, 226, **228**, 240, 242, 256	+ 2H + CO_2
P8	421.1176	421.1183	-1.6	$C_{26}H_{17}N_2O_4$	212	2-OH-AC dimer

[a] Calculated using Molecular Mass Calculator freeware version v2.02.

Table 3

MS/MS collision-induced dissociation of glutathione S-conjugate			2-OH-AC		
			Measured *m/z* / Da	Calculated *m/z* / Da [a]	Deviation / ppm
Neutral losses	Parent	*m/z* / Da	517.1382	517.1387	1.04
	Glycine	75.0320	None	442.1067	None
	Anhydroglutamic acid	129.0426	388.0963	388.0962	-0.39
	Glutamine	146.0691	None	371.0696	None
	γ-Glu-Ala-Gly	275.1117	244.0421 [b]	244.0427	2.34
	Glutathione (S-oxide)	322.0709	None	195.0679	None

[a] Calculated using Molecular Mass Calculator freeware version v2.02.
[b] Neutral loss of γ-Glu-Ala-Gly + 2H.

Figure

Cyclic voltammograms of 0.5 mM 2-OH-AC and 5 mM GSH alone and in the mixture in 0.02 M PBS buffer, pH 7.40. Experimental conditions: potential range -0.2 – 1.2 V; scan rate 100 $mV \cdot s^{-1}$; T = 21 ^{o}C; ϕ GC 3 mm (supplemental data for Figure 2).

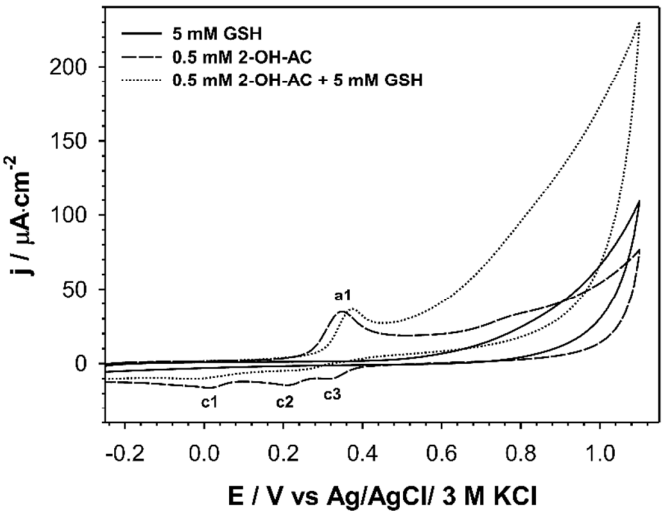

Figure

The representative high performance LC chromatograms of the control incubations prepared for enzymatic oxidation of 2-OH-AC in RLMs (supplemental data for Figure 6a).

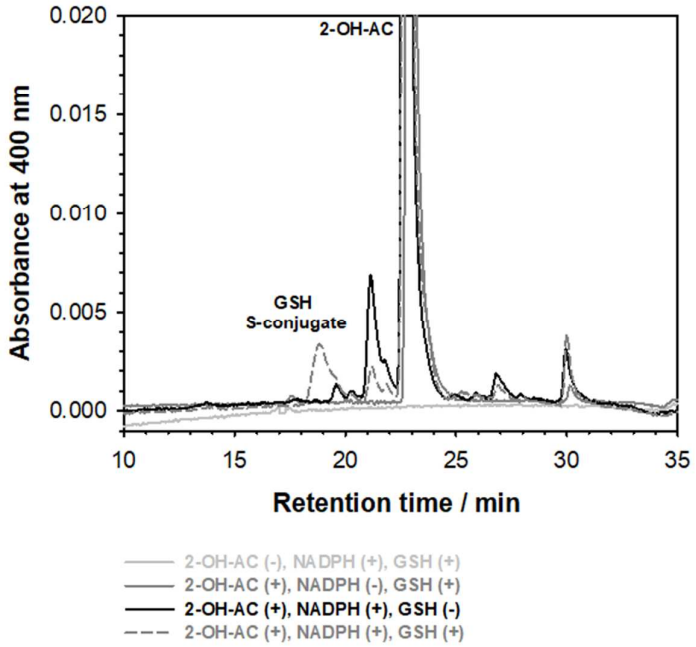

Table

A summary of the electrochemical products observed under different electrolyte conditions.

	Electrolyte composition		
Product / *m/z* / Da	(1) 0.1% formic acid in water/methanol (50/50, *v/v*)	(2) 0.1% formic acid in water/acetonitrile (50/50, *v/v*)	(3) 20 mM ammonium formate (pH 3.40) in water/acetonitrile (50/50, *v/v*)
P1 / 226	+[a]	+[a]	++[b]
P2 / 227	++[b]	+[a]	+[a]
P3 / 228	+[a]	**++**[b]	**++**[b]
P4 / 240	**++**[b]	ND[c]	ND[c]
P5 / 242	**++**[b]	+[a]	+[a]
P6 / 256	+[a]	+[a]	**++**[b]
P7 / 258	+[a]	+[a]	+[a]
P8 / 421	+[a]	ND[c]	ND[c]

Ions showing the highest intensity in a given electrolyte are shown in bold. [a] +: low intensity, [b] ++: high intensity, [c] ND: not detected.